ISSN: 2165-3259

JAOCR

Official Journal of the American Osteopathic College of Radiology

BRAINS & BONES

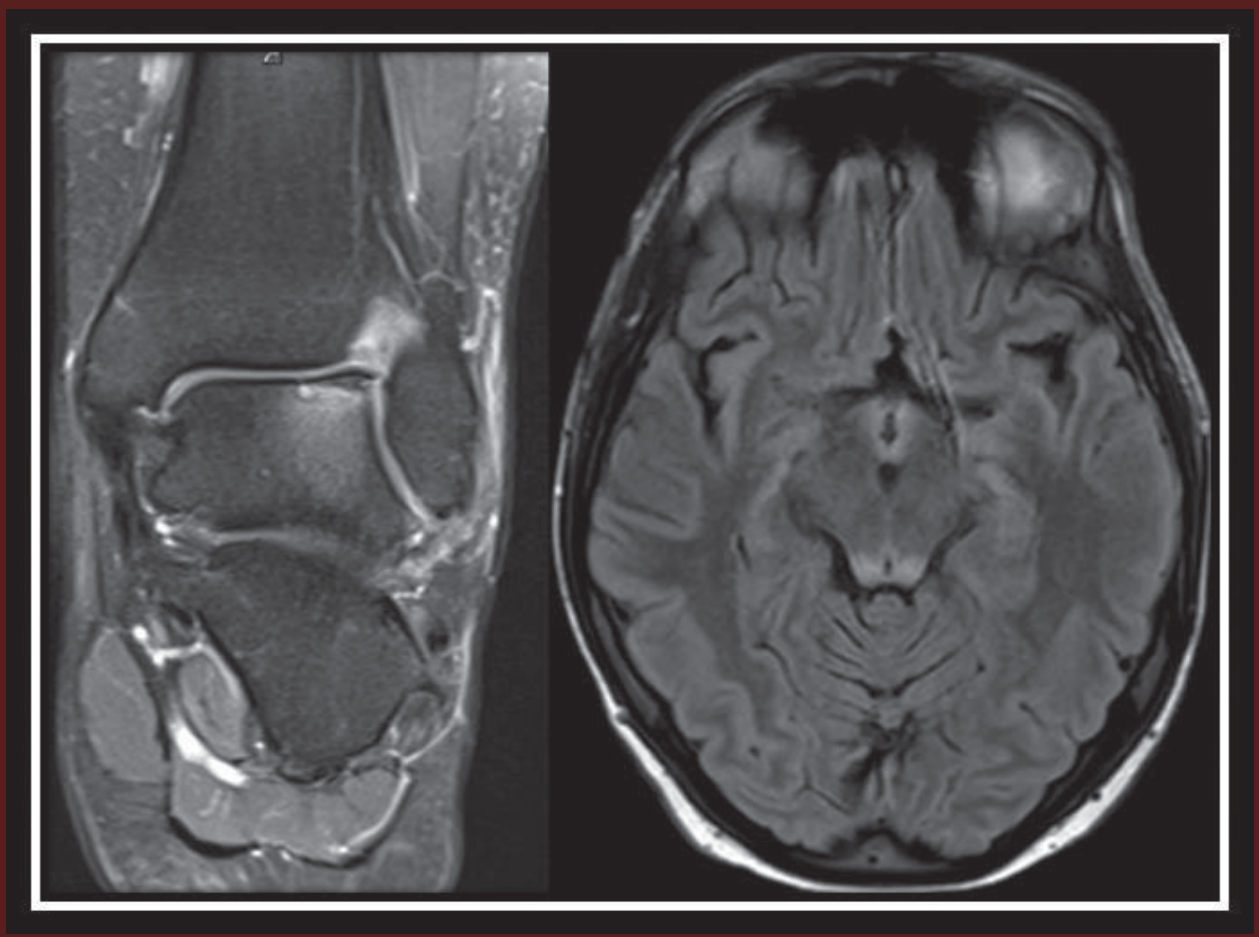

Editor-in-Chief: William T. O'Brien, Sr., D.O.

April 2015, Vol. 4, Issue 2

JAOCR

Official Journal of the American Osteopathic College of Radiology

Aims and Scope

The Journal of the American Osteopathic College of Radiology (JAOCR) is designed to provide practical up-to-date reviews of critical topics in radiology for practicing radiologists and radiology trainees. Each quarterly issue covers a particular radiology subspecialty and is composed of high quality review articles and case reports that highlight differential diagnoses and important teaching points.

Access to Articles

All articles published in the JAOCR are open access online. Subscriptions to the journal are not required to view or download articles. Reprints are not available.

Copyrights

Guide for Authors

Submissions for the JAOCR are by invitation only. If you were invited to submit an article and have questions regarding the content or format, please contact the appropriate Guest Editor for that particular issue. Although contributions are invited, they are subject to peer review and final acceptance.

Editor-in-Chief

Associate Editor

Editorial Board

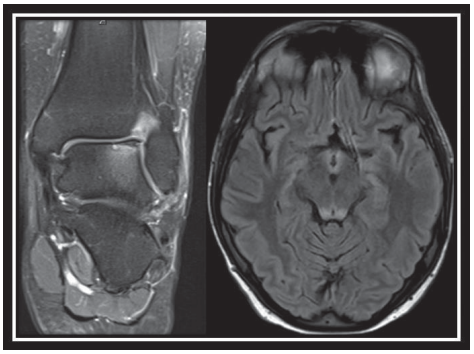

JAOCR

BRAINS & BONES

Editor: William T. O'Brien, Sr., D.O.

From the Editor

Review Articles

Differential-Based Case Reviews

JAOCR at the Viewbox

"The brain is a wonderful organ; it starts working the moment you get up in the morning and does not stop until you get into the office."

— Robert Frost

In this Issue

William T. O'Brien, Sr., D.O.

Editor-in-Chief, *Journal of the American Osteopathic College of Radiology*

It is a pleasure to present the latest issue of the JAOCR, especially to those who may be reading the journal for the first time. The JAOCR is a quarterly journal that has been in publication since 2012. The journal was initially developed as an educational resource for the members of the college (AOCR), publishing a series of review articles and differential-based case reports covering a particular radiology subspecialty; however, as this journal is now open access with Anderson Publishing, it has become available to the radiology community-at-large.

For each issue of the JAOCR, guest editors are invited to recruit contributors and content in their particular subspecialties. The guest editors review and edit each issue prior to submission to the JAOCR. Although invited, articles undergo additional peer review to ensure the highest quality content in the journal.

Submission of articles is by invitation only through the guest editors. If you would like to be considered for a guest editor position in a particular subspecialty field, please contact the AOCR staff at info@aocr.org with your contact information, subspecialty of interest, and a copy of your CV. All radiologists are welcome to serve as contributors, and AOCR membership is not a requirement for participation in the journal.

This issue of the JAOCR is titled *Brains & Bones* with articles on neuro- and musculoskeletal imaging. The format for this issue was inspired by the 2013 mid-year AOCR conference in Dallas, TX, which was chaired by Dr. Rocky Saenz.

For the MSK portion of this issue, Drs. Saenz, Ries, Giese, and Knapp from Botsford Hospital in Farmington Hills, MI, authored a comprehensive review article on MRI of the ankle and hindfoot; Drs. Kotecha and Cerniglia from the University of Massachusetts Memorial Medical Center in Worcester, MA, put together a differential-based case report reviewing lytic epiphyseal lesions; and Drs. Sheeler and Saenz from Botsford Hospital authored a Viewbox article showing an unstable osteochondral defect.

For the neuroimaging portion of the issue, I drafted a pictorial review article covering the CNS imaging manifestation of neurofibromatosis Type 1; Dr. Zapadka of Wake Forest Baptist Health in Winston-Salem, NC, authored a comprehensive case-based review of temporal lobe signal abnormality on MRI; and Dr. Betts of Cincinnati Children's Hospital Medical Center in Cincinnati, OH, composed a Viewbox article on Wernicke encephalopathy.

I wish to express my deepest gratitude to the contributors of this issue for volunteering their time and expertise to put together an exceptional educational resource. I hope that you thoroughly enjoy this and future issues of the JAOCR.

The views expressed in this material are those of the author, and do not reflect the official policy or position of the U.S. Government, the Department of Defense, or the Department of the Air Force.

MRI of Ankle and Hindfoot Pain

Rocky Saenz D.O., Stacy Ries, D.O., Juliann Giese, D.O., Daniel Knapp D.O.

Department of Radiology, Botsford Hospital, Farmington Hills, MI

Over the last 10 years, there has been a significant increase in ankle MRI. When patients present to their primary care physician or specialist with ankle or hindfoot pain, there are a variety of possible etiologies. Unfortunately, these different diagnoses have overlapping clinical signs and symptoms. For this reason, referring clinicians tend to rely on MRI to clarify or solidify a diagnosis to guide treatment and management decisions. Therefore, it is important for the radiologist to be able to recognize and diagnose common pathologies within this region. This review article focuses on ligamentous injuries, common tendon pathology, and overuse syndromes.

Ligamentous injuries

Lateral Ligamentous Injuries

Ankle joint injuries are the most common sports-related injuries with approximately 75% involving the lateral ligamentous complex.1 The lateral complex is composed of the anterior talofibular ligament (ATF), the calcaneofibular ligament (CF), and the posterior talofibular ligament (PTF).1 The anterior talofibular ligament is the most commonly injured ligament as it is the weakest of the lateral ankle ligaments, followed by the calcaneofibular ligament and finally the posterior talofibular ligament.[1-3] These ligaments are almost always injured sequentially from anterior to posterior. Therefore, if the ATF is intact on imaging, it can often be presumed that the other lateral collateral ligaments are also intact.[4]

Nearly half of ATF injuries occur during an athletic activity with basketball being the most commonly involved sport.[5] The classic mechanism of injury is ankle inversion with forced plantar flexion. Patients typically present with acute lateral ankle pain and soft tissue swelling.[1,6] Clinicians evaluate the degree of swelling, ecchymosis, and inability to bear weight to assess the grade/extent of ligamentous injury.[1,6] Teenagers and young adults experience the highest rates of ankle sprains with an equal incidence among males and females.[1,3,7]

The mainstay treatment for acute ligamentous ankle injury is conservative management with short-term immobilization, followed by functional rehabilitation. A successful recovery occurs in approximately 80% of patients utilizing this approach.[1,3,7] Since treatment rarely requires surgical intervention, MRI is typically reserved for evaluating highly competitive athletes in whom primary ligamentous repair is being considered, as well as for the 20% of patients who develop chronic ankle instability following failed conservative treatment.[1-3, 7]

When evaluating the lateral ligaments, both the axial and coronal images are useful. Axial images demonstrate the ATF and PTF more clearly, while coronal images better demonstrate the calcaneofibular ligament. MRI findings of acute ATF injury include ligament discontinuity, nonvisualization of the ligament, detachment, and/or contour irregularity.[2-4] Indirect associated findings for an ATF injury include loss of surrounding fat planes, ankle joint effusion, and lateral soft tissue edema.[2-4] In addition, the presence of a "bright rim" sign (a bright dot-like or curvilinear high-signal intensity focus on T2 images involving the talus and fibula along the cortex) significantly increases the accuracy of detecting ATF injuries.[3] A complete tear is typically seen on MRI as a fluid-gap/discontinuity with subsequent retraction of lax fibers or nonvisualization of the ligament (**Figure 1**).[7]

Medial Ligamentous Injuries

The deltoid ligamentous complex, also known as the medial collateral ligament, is the strongest of the ankle ligaments. It serves as the primary stabilizer of the axially loaded ankle.[6,8] Unlike its lateral counterpart, it is rarely injured, accounting for only 5% of all ankle sprains. Male athletes are 3 times more likely to experience a

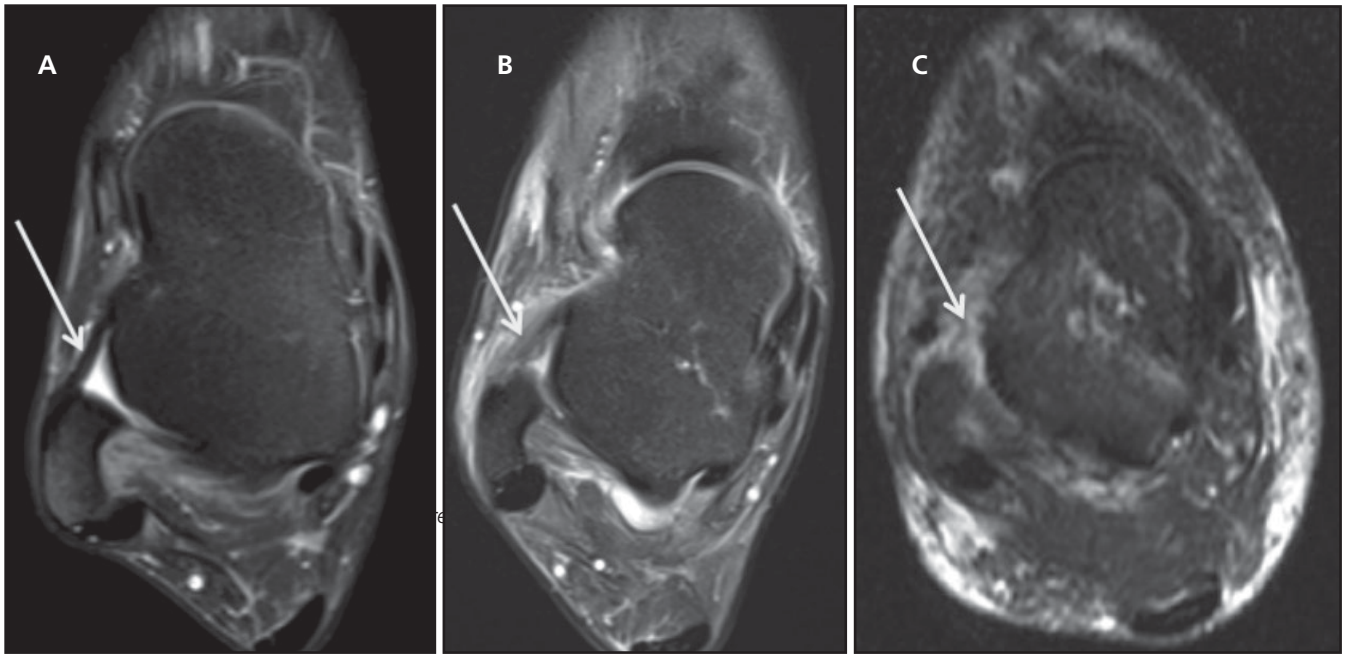

FIGURE 1. *ATF normal, partial tear, complete tear. Axial proton density fat-saturated (PD FS) image (A) shows the normal appearance of the ligament (arrow). Axial PD FS image (B) displays abnormal thickening of the ATF (arrow). Axial PD FS image (C) demonstrates nonvisualization of the anterior talofibular ligament with extensive surrounding soft tissue edema involving the anterior aspect of the lateral gutter (arrow) compatible with ATF complete tear.*

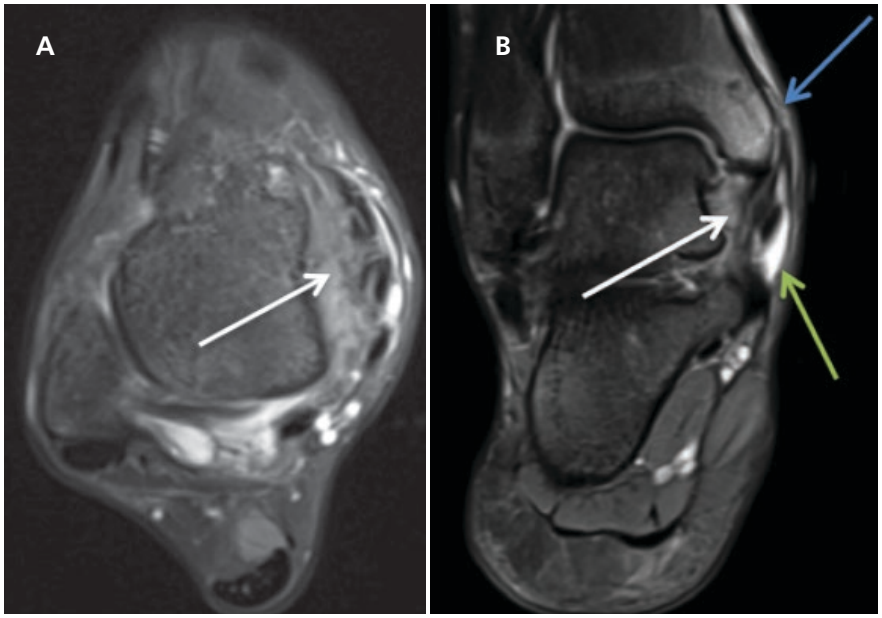

FIGURE 2. *Deltoid sprain. Axial (A) and coronal (B) PDFS images demonstrate increased signal intensity within thickened deltoid ligament deep fibers (white arrows) compatible with deltoid sprain. Patchy high-intensity signal is seen involving the medial malleolus (blue arrow) revealing an associated medial malleolus contusion. Fluid is seen within the posterior tibial tendon sheath with an otherwise normal-appearing tendon (green arrow), consistent with tenosynovitis.*

medial ankle sprain than females.[6-9] Forced eversion and pronation of the ankle is the classically described mechanism of injury, most often resulting in a medial malleolus avulsion fracture due to the strength of the deltoid ligament.[6,8] Medial ankle sprains are more painful than lateral ankle sprains and often result in mechanical instability.[7] Patients commonly present with medial ankle hematoma and tenderness in the acute setting.[8]

The deltoid ligament is comprised of 2 obliquely oriented, parallel components (superficial and deep), which join together to form the triangular/deltoid-shaped ligamentous complex.[6-9] These 2 components act somewhat synergistically to stabilize the ankle against valgus and pronation forces.[8] The most superficial component is comprised of the tibiocalcaneal, tibionavicular, posterior superficial tibiotalar, and tibiospring ligaments. The deep group consists of the anterior tibiotalar ligament and posterior deep tibiotalar ligaments (PDTL).[8] Tears involving the deep ligaments are more common; however, tears of both layers rarely occur in isolation. Injuries to these two components should be classified separately on MRI.[7,8,10]

When evaluating the deltoid ligament, the coronal images are typically the easiest to use. The most common MRI findings of acute deltoid ligament sprain include fascicular disruption, heterogeneity, and loss of striations within the ligament.[10] An acutely torn ligament is best appreciated on fluid-sensitive, fat-saturated sequences in the coronal plane, which demonstrate increased

fluid signal with fluid-filled gaps or complete discontinuity of the ligament (**Figure 2**).[7,10] The deep PDTL is generally regarded as the thickest and strongest of the ligaments and normally demonstrates a heterogeneous appearance with internal striations caused by individual fascicles separated by interposed fat; acute injury causes this ligament to become amorphous with loss of these striations secondary to hemorrhage and hemosiderin deposition.[7,10] Treatment of deltoid ligament injuries remains somewhat controversial with surgical treatment being primarily reserved for those with associated fractures, chronic deltoid ligament injury, and/or chronic ankle instability.[8,10]

Tendon Injuries

Imaging Tendons

Tendons should have a homogeneous hypointense appearance on MRI. Specifically, T1-weighted (T1W), T2-weighted (T2W), proton density (PD), and inversion recovery (IR) images should all demonstrate homogeneous hypointense signal intensity throughout the tendons. The Achilles tendon is the one exception to this rule within the ankle (see Achilles discussion below). Since the Achilles tendon is a conglomeration of tendons, it often has some small foci of intermediate intratendinous signal intensity. When reviewing an MRI, the best approach is to follow each tendon from the most cranial image to the most caudal image, evaluating them for homogeneity with regard to shape and signal intensity. It is the opinion of the authors that the axial plane provides the easiest approach for evaluating tendons of the ankle.

Tendon Abnormalities

The major abnormalities involving tendons include degeneration, tenosynovitis, partial tears, complete tears, tumors, and a multitude of deposition disorders within the tendon. Degeneration of a tendon occurs from aging or chronic overuse. Generally, this is a painless process but may evolve or predispose the tendon to partial or complete rupture with relatively minimal trauma. Tendons with degeneration will exhibit a normal or enlarged caliber with intermediate signal intensity within the substance of the tendon (centrally) on T1 sequences and corresponding hyperintense T2 signal. Tendinitis, tendinopathy or tendinosis are all used to describe abnormal intratendinous signal. On imaging, it is difficult or impossible to distinguish signal intensity of degeneration from partial tears, and both processes are thought to be on a continuum of microtear progression.[11]

Tenosynovitis refers to fluid surrounding the tendon, which indicates an inflammatory process of the tendon sheath. The underlying tendinous substance can be of normal or abnormal signal intensity. Fluid signal intensity (hypointense T1/hyperintense T2) must surround the entire circumference of the tendon to diagnose tenosynovitis.

A partial tear represents incomplete disruption of the tendon fibers, whereas a complete tendon tear/rupture results in total disruption of the tendon with 2 distinct ends of the tendon identified. Partial tears can be variable in appearance on MRI but typically exhibit high signal intensity within the tendon substance on fluid sensitive sequences. Chronic tears may have low T2 signal intensity due to scarring and fibrosis. The tendon may appear thickened, thinned, or of normal caliber depending on the etiology and age of the injury. A tear may occur in a vertical or longitudinal fashion with respect to the long axis of the tendon.

A complete rupture is easier to identify on clinical examination secondary to dysfunction or severe weakness. The role of imaging is to confirm the presence of a full thickness tear, determine the quality of tendon remnants, and identify the degree of retraction. These factors are important for patient management and surgical planning.[11]

Achilles Tendon Injuries

Achilles tendon pathology is a common cause of hindfoot pain. In the past 3 decades, the incidence has increased secondary to increased participation in recreational and competitive sports.[12] The rate of Achilles tendon injuries in runners is approximately 10 times higher than in age-matched controls.[13] The most common patients who suffer from this condition are physically active individuals who have recently increased their training regimen, resulting in repetitive microtrauma. The peak age of occurrence is 30-40 and with a slight male predominance.[14] As the largest tendon in the body, the Achilles tendon endures strain and is at risk of rupture from running, jumping, and sudden acceleration and deceleration movements.[14] Achilles tendon injury can be associated with trauma at any age, and physical examination findings typically differentiate between partial and complete rupture.[14]

Achilles tendon rupture presents with an acute onset of severe pain, often described as "being kicked" or "shot in the heel."[12] In contrast, pain associated with tendinopathy generally occurs at the beginning and end of a training session with variable periods of discomfort during activity.[13] Tendon injuries can be acute or chronic. In the acute phase, the tendon becomes edematous with maximal tenderness to palpation approximately 2-6 cm proximal to the insertion point on the calcaneus.[13] Patients will have difficulty with active plantar flexion of the foot. The "Thompson test" or squeezing of the calf muscle with the patient in a prone position assesses the integrity of the Achilles tendon. If intact, calf squeeze will result in passive plantar flexion. In the setting of Achilles rupture, however, the test will not result in passive plantar flexion.[14]

The Achilles tendon represents a confluence of the gastrocnemius and soleus muscles that end in a tendinous insertion on the superior calcaneal tuberosity.[13] The tendon most commonly has a flat or concave anterior margin on axial images; however, a focal convexity may be seen as a normal variant in some individuals. This focal anterior contour convexity is caused by the soleus muscle

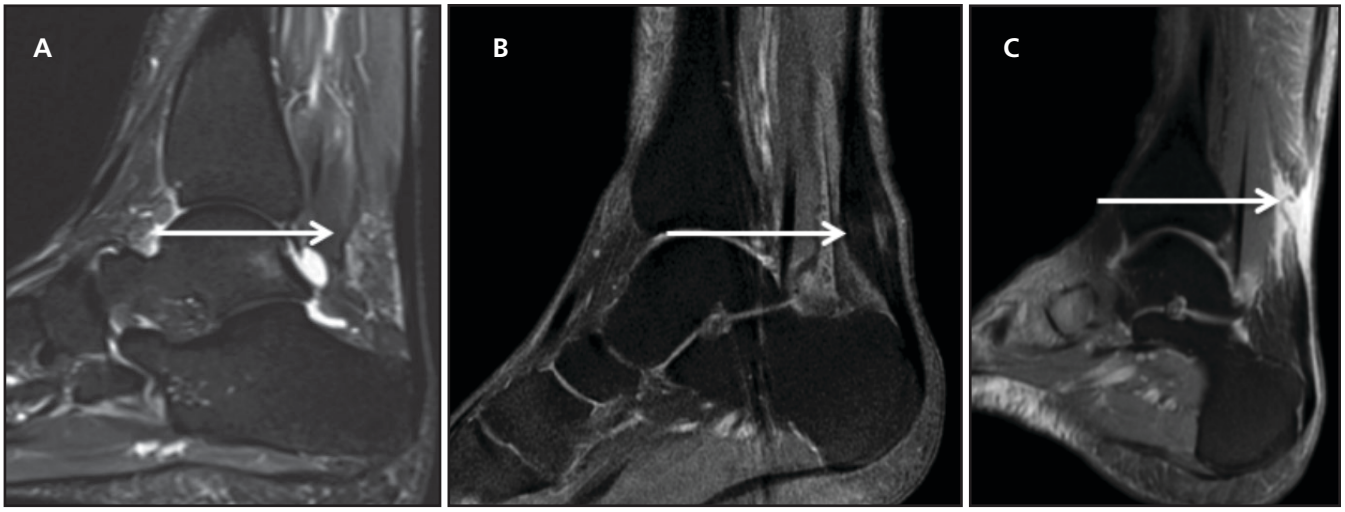

FIGURE 3. *Achilles tendon: Normal, intrinsic partial tear, and rupture. Sagittal inversion recovery (IR) image (A) shows a normal tendon (arrow). Sagittal IR image (B) shows a focal thickened tendon with an intrinsic partial tear, pregnant Achilles sign (arrow). Sagittal PD FS image (C) demonstrates a "fluid gap" (arrow) associated with tendon rupture*

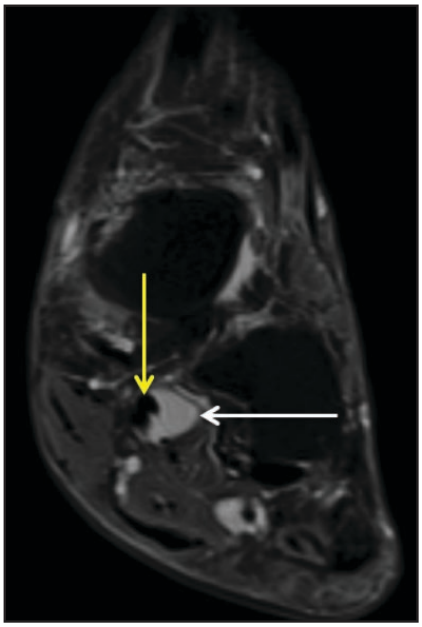

FIGURE 4. *Master knot of Henry bursitis. Coronal PD FS shows fluid signal surrounding the master knot of Henry (midfoot junction at crossing between FHL & FDL). The image shows the FHL superiorly (yellow arrow) and FDL inferiorly surrounded by focal fluid (white arrow).*

fibers merging with the gastrocnemius muscle in a spiral configuration.[11] The tendon does not have a surrounding true synovial sheath, as is the case with the remaining tendons of the ankle; rather, it has a paratenon composed of a single layer of cells. This surrounding tissue is highly vascularized and is responsible for much of the blood supply to the tendon. Approximately 12-15 cm from its insertion point onto the calcaneus, the fibers begin to rotate at 90 degrees, and this rotation becomes most pronounced at approximately 5-6 cm from the insertion. Angiographic injection studies have demonstrated a zone of relative hypovascularity 2-7 cm proximal to the insertion point. This predisposes the distal aspect of the tendon (approximately 4-6 cm proximal to the calcaneal insertion) to injury with a relative inability to properly heal.[11,13]

The Achilles tendon is easiest to evaluate utilizing both the sagittal and axial planes. The sagittal plane demonstrates continuity of a normal tendon with a uniform slender appearance (**Figure 3A**). Acute partial thickness injury will manifest as edema and hemorrhage, which is seen as increased intra-tendinous T2 signal intensity. In addition, the aforementioned flat to concave anterior margin will appear convex anteriorly, which is best seen on the axial images. A focal anterior bulge may be seen with both tendinosis and partial tears on sagittal sequences (**Figure 3B**). In the setting of complete tendon rupture, the most reliable imaging finding is identifying tendon discontinuity (**Figure 3C**). When viewed in the sagittal plane the degree of retraction may also be evaluated which is important for surgical planning. A complete tear or rupture generally requires surgical intervention, while a partial tear may be amenable to conservative therapy.[11]

Flexor Hallucis Longus Tenosynovitis

The medial compartment tendons of the ankle from anterior to posterior include the posterior tibialis, flexor digitorum, and flexor hallucis longus (remembered as Tom, Dick and Harry). Flexor hallucis longus (FHL) tenosynovitis is commonly referred to as "dancer's tendinitis" due to its high prevalence among professional female ballet dancers.[15,16] Chronic, repetitive, forced plantar-flexion, such as en-pointe dancing, creates irritation and inflammation of the flexor hallucis longus tendon sheath as it enters the flexor retinaculum. This leads to the development of tenosynovitis, the most common FHL-related injury.[15,16] Patients classically present with insidious onset posteromedial ankle pain that is worsened by activity.[16] The hallmark physical exam finding is pain with active hallux plantar flexion against resistance.[16,17]

Tenosynovitis most commonly occurs proximally, posterior to the talus, at the level of the sustenaculum talus as the tendon descends into the fibro-osseous tunnel between the medial and lateral talar tubercles.[2,17,18] Symptoms,

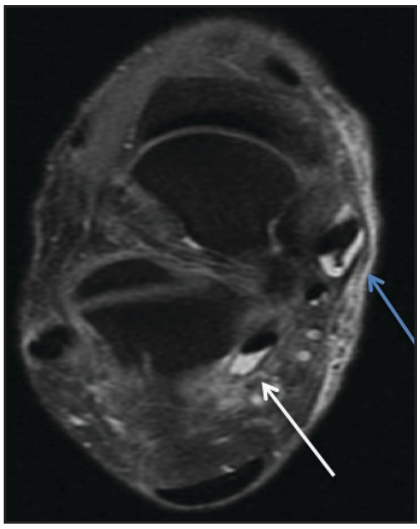

FIGURE 5. *Tenosynovitis of the FHL and posterior tibialis tendons. Axial PD FS image demonstrates fluid signal intensity surrounding the flexor hallucis longus tendon with an otherwise normal-appearing, homogenous tendon (white arrow). A similar appearance is noted involving the posterior tibialis tendon (blue arrow) also consistent with tenosynovitis.*

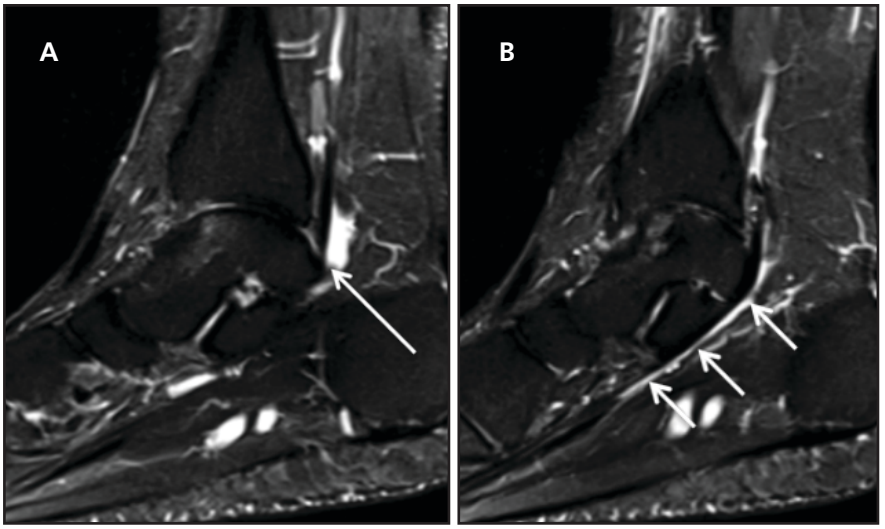

FIGURE 6. *FHL tenosynovitis. Sagittal IR image (A) demonstrates focal fluid signal within the tendon sheath surrounding the FHL tendon at the level of the ankle joint (arrow). Next contiguous sagittal IR image (B) demonstrates fluid extending below the level of the ankle joint (arrows) with an otherwise normal tendon compatible with FHL tenosynovitis. Note there is no significant ankle joint effusion present.*

however, may occur anywhere throughout its course, including the midfoot at the master knot of Henry and distally within the forefoot between the sesamoids at the region of the FHL tendon insertion.[2,17,18] Therefore, it is essential for the radiologist to follow the FHL tendon from its origin to its insertion in order to avoid overlooking less common but symptomatic locations of irritation. One of these uncommon areas is at the knot of Henry (**Figure 4**). The master knot of Henry is the midfoot tendinous junction or crossing between the flexor hallucis longus and flexor digitorum longus,[19] originally described by Henry. There is typically FHL tenosynovitis proximal to the master knot. Various additional pathologies have been described in association with FHL tenosynovitis, such as posterior ankle impingement, which may be caused by a mobile os trigonum or Stieda's process (see section on os trigonum syndrome), synovial adhesions, tendon hypertrophy, distal insertion of the FHL muscle, muscle elongation, longitudinal degenerative tears, and nodularity within the fibro-osseous tunnel.[16,17]

MRI is often ordered if there is a high clinical suspicion for posterior impingement or FHL tenosynovitis.[16] One study demonstrated 82% of patients with suspected FHL tenosynovitis had positive MRI findings, revealing excess fluid accumulation within the FHL tendon sheath posterior to the ankle joint (**Figure 5**).[16] A potential pitfall is a normal communication between the FHL tendon sheath and tibiotalar joint that exists in approximately 20% of individuals. Care should be taken not to mistake physiologic synovial fluid occurring within the tendon sheath in these individuals with pathology (**Figure 6**).[2, 20]

Conservative treatment with physical therapy and anti-inflammatory medication is often the appropriate initial treatment for FHL tenosynovitis. Surgical intervention is typically reserved for high-level athletes and performers unable to perform desired activities or in the setting of failed conservative management.[16] The surgical technique utilized for FHL tenosynovitis is tendon sheath release.[16]

Posterior Tibial Tendon Injury

The posterior tibial tendon (PTT) is the largest tendon within the medial compartment and is approximately twice the size of the others (flexor digitorum and flexor hallucis longus). The PTT passes inferior and posterior to the medial malleolus and uses the medial malleolus as a pulley. The PTT attaches to the navicular bone, the 3 cuneiforms, and the bases of the first through fourth metatarsals. A potential pitfall in evaluating this tendon is the multiple sites of attachment and orientations of the multiple tendinous branches. The attachment sites often have a thickened appearance and high signal intensity, which is a normal finding and should not be confused with a partial tear, especially at the navicular attachment site.[11]

High signal intensity or tendinous thickening elsewhere in the tendon, however, is considered pathologic. Hyperintense intrasubstance T2 signal intensity indicates a partial tear (**Figure 7**). Commonly, this will be evident as the tendon passes posterior to the medial malleolus, as this is a site of bony compression with a forced eversion type injury.[21] A small amount of fluid may be present eccentrically around a normal tendon. If fluid is seen completely encompassing the tendon, this implies a tenosynovitis. A high association of PTT dysfunction is

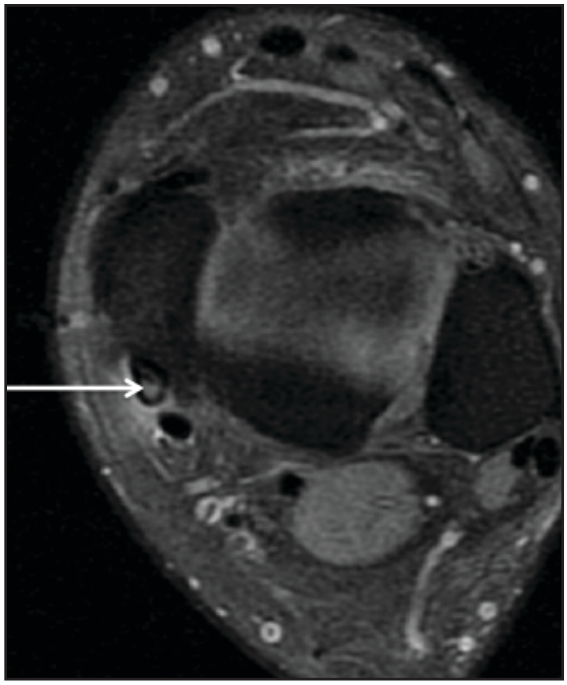

FIGURE 7. *Posterior tibial tendon partial tear. Axial PD FS image demonstrating increased tendon size, surrounding edema, and abnormal intrinsic signal (arrow).*

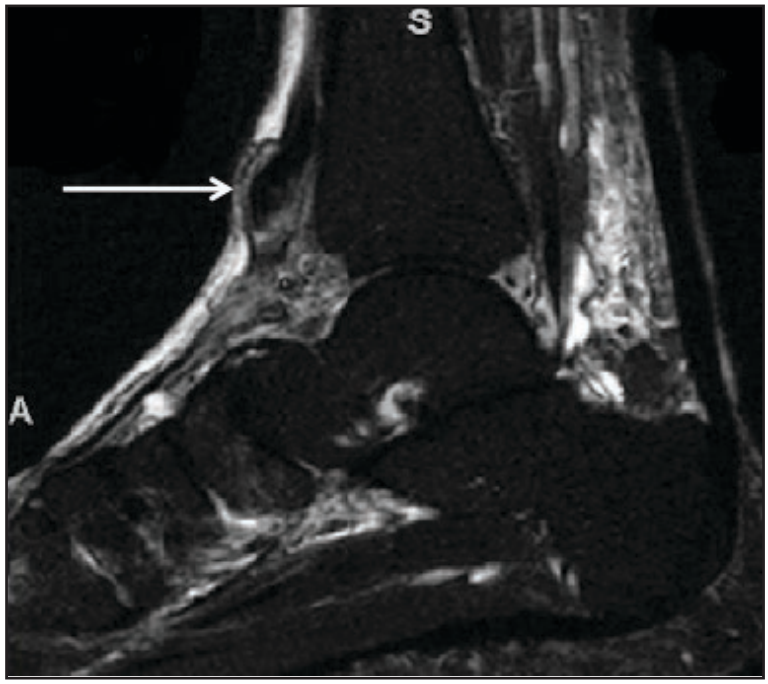

FIGURE 8. *Anterior tibial tendon rupture. IR sagittal image demonstrates a focal mass in the anterior ankle, which represents the retracted anterior tibialis tendon (arrow). There is loss of signal of the normal subcutaneous fat signal intensity secondary to edema.*

associated with abnormalities of the navicular bone, to include os naviculare, and will be discussed in more detail elsewhere in this article.

Anterior Tibial Injury

Classically, 3 tendons are found in the anterior compartment of the ankle. From medial to lateral, these are the anterior tibial, extensor hallucis longus, and extensor digitorum longus (can be remembered as "Tom's Hairy Dog"). These tendons are responsible for dorsiflexion of the ankle and foot. The anterior tibial tendon is the most likely of all of the anterior compartment to be pathologic. This tendon is the most medial and the largest of the anterior tendons. It begins at approximately the junction between the lower and middle third of the tibia and courses inferiorly to the medial border of the foot, inserting on the first metatarsal base and first cuneiform. Throughout its course, it is held tightly to the ankle joint by three retention tunnels formed by the superior extensor retinaculum and the superior-medial and inferiomedial limbs of the inferior extensor retinaculum.[23]

Trauma is a common cause of anterior tibial tendon injury. Non-traumatic tears are uncommon, but may be seen with increasing age and in individuals who run on inclines. Rupture can result in a significant degree of dysfunction with diminished ankle dorsiflexion strength. Occasionally, patients with a partial or complete tear of this tendon present with a focal mass suspected to be a tumor, rather than with symptoms of a tendon injury, but most are diagnosed clinically prior to imaging.[11] On physical exam, weak dorsiflexion of the ankle with maintained hyperextension of the hallux and lesser digits will be evident.[24]

The role of imaging with a complete anterior tibial tendon rupture is for confirmation, to detect other tendinous injuries, to evaluate the extensor retinaculum, and for surgical planning. The classic MR findings of any tendon rupture is discontinuity of the tendon, thickening of the retracted portion, and excess fluid in the tendon sheath (**Figure 8**).[24]

Nonsurgical treatment includes bracing and is reserved for the elderly or cases in which surgery will not be tolerated secondary to medical comorbidities.[25]

Peroneus Brevis Partial Tear

The lateral compartment tendons of the ankle include the peroneus brevis and longus (also known as the fibularis brevis and longus), which serve as the primary evertors of the foot. Together, they pass posterior and inferior to the lateral malleolus and use this bony prominence as a pulley. A common tendinous sheath is shared in the proximal fibula; the tendons and sheath then separate distally to become 2 distinct tendons. The peroneus brevis attaches to the base of the fifth metatarsal. The peroneus longus splays out to attach on multiple sites along the plantar aspect of the foot, mainly involving first cuneiform and first metatarsal. Normally, the peroneus brevis is flat or oval shaped. It is situated posterior to the lateral malleolus and anterior to the peroneus longus.

"Peroneus brevis split" is used to describe a longitudinal or vertically oriented tear, which is the most common injury of the peroneus brevis tendon.

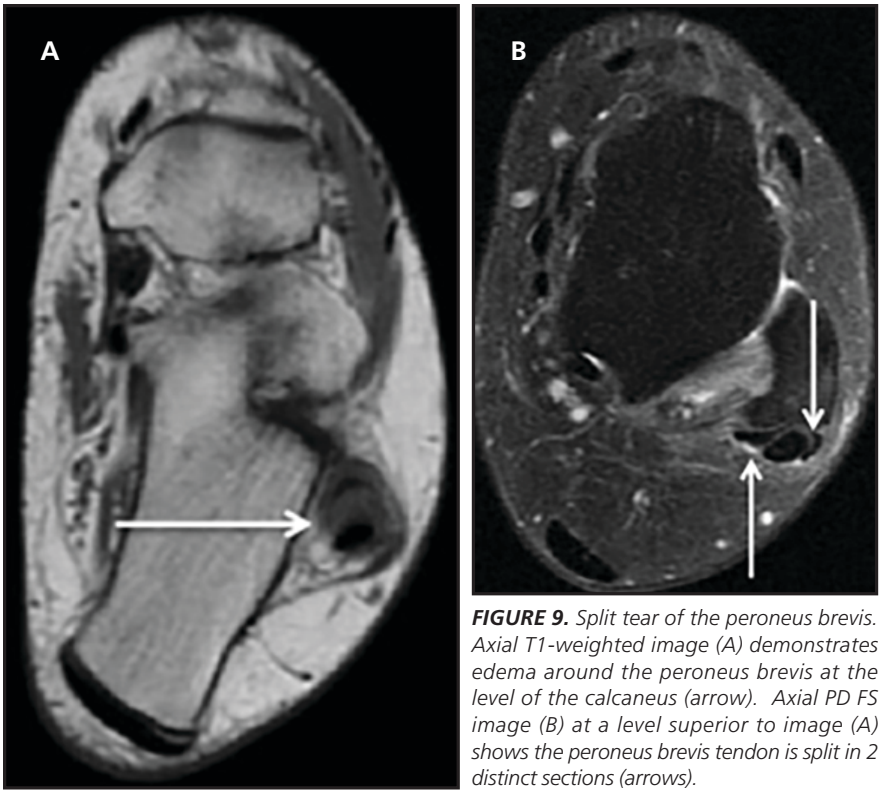

FIGURE 9. *Split tear of the peroneus brevis. Axial T1-weighted image (A) demonstrates edema around the peroneus brevis at the level of the calcaneus (arrow). Axial PD FS image (B) at a level superior to image (A) shows the peroneus brevis tendon is split in 2 distinct sections (arrows).*

A history of severe or recurrent inversion type ankle injury is usually elucidated. Lateral ankle pain and edema along the course of the tendon is generally evident clinically. Multiple structures, to include the lateral collateral ligaments, have a high association of injury with peroneus brevis injuries, and many symptoms overlap with chronic ankle instability.[11] During forced dorsiflexion, the peroneus brevis tendon is compressed between the peroneus longus and the lateral malleolus, resulting in a vertical tear. The key findings of a split tear on MRI include identifying the peroneus brevis tendon separated into 2 distinct tendons (**Figure 9**).

Overuse Injuries/Syndromes

Os Trigonum Syndrome

Also known as posterior impingement syndrome, os trigonum syndrome (OTS) presents as acute or chronic posterior ankle pain exacerbated by both plantar and dorsiflexion. Along with other ankle impingement syndromes, OTS is most commonly seen in dancers and soccer players.[26,27] The name os trigonum syndrome infers causation of a prominent os trigonum (an unfused accessory ossicle of the lateral tubercle of the talus), but this is only one of the anatomic etiologies. Other predisposing anatomic variants include a prominent lateral talar tubercle termed "Stieda's process" (a shelf-like superior prominence of the calcaneal tuberosity), prominent down-sloping of the posterior tibial articular surface, and a posterior intermalleolar ligament.[28,29] Soft-tissue causes of impingement can also occur and may be attributed to synovitis of the flexor hallucis longus tendon sheath, a thickened posterior intermalleolar ligament, posterior synovial recess of the subtalar and tibiotalar joints, disruption of the synchondrosis between the os trigonum and the lateral talar tubercle, or loose bodies.[28-34]

An os trigonum may be present in up to 14% of asymptomatic patients.[32] Therefore, MRI is critical in assessing for findings of OTS, including bone marrow edema, posterior ankle soft tissue inflammatory changes, a thickened posterior intermalleolar ligament, and posterior ankle synovitis (**Figure 10**). Inflammatory changes are specifically seen in the posterior synovial recess of the subtalar and tibiotalar joints.[29] Synovitis of the flexor hallucis longus is also commonly seen. Additional imaging findings on MRI include posterior capsular thickening, bone marrow edema or fluid signal at the synchondrosis, and ligament disruption. After diagnosis of OTS, conservative management, which may include image-guided steroid injection, is the first line of treatment. If conservative management fails, arthroscopic resection of the os trigonum or other associated abnormalities is performed.

Os Naviculare Syndrome

Os naviculare syndrome is generally classified as a chronic stress related injury. Although there is no classic patient population, the symptoms of os naviculare syndrome become more pronounced during weight-bearing, walking, repetitive activities, and when wearing narrow shoes.[35] There are three types of accessory navicular bones that are classified based on their shape and location. Type I is located in the distal portion of the posterior tibial tendon, measuring 2-3 mm and is usually asymptomatic. Type II is most important clinically as it is present in up to 4%-21% of the population and is commonly associated with medial bone pain.[36] Considered the secondary ossification center of the navicular bone, a type II accessory navicular bone resides slightly posterior to the medial pole of the navicular bone (**Figure 11**). This accessory bone has also been referred to as a "prehallux." Type III is sometimes referred to as a fused Type II and relates to a prominent navicular tuberosity. Further discussion relates to Type II accessory navicular bones, as it is the most common type to cause pain.

Repetitive actions may cause shearing stress forces at the ossicle-navicular synchondrosis. Since all or portions of the posterior tibial tendon insert on the accessory ossicle, this may lead to tenosynovitis of the posterior tibial tendon, tendon disruption, granulomatous inflammation, soft tissue swelling, and/or a mass of fibrocartilage tissue. Sequelae

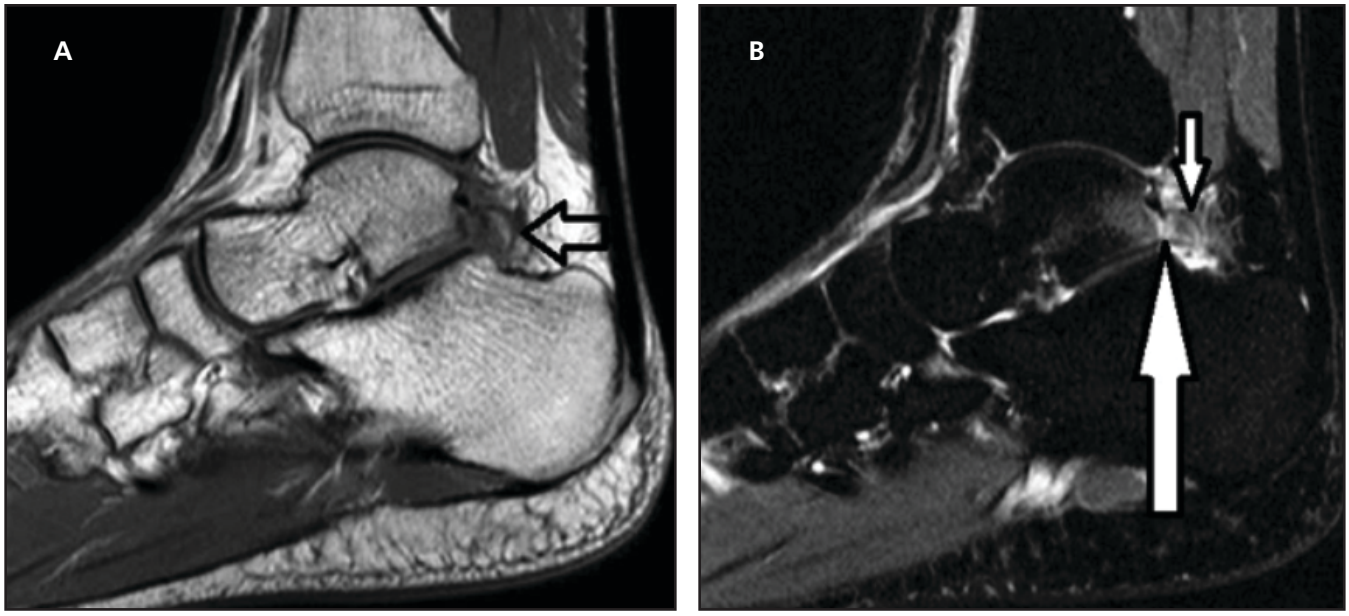

FIGURE 10. *Os trigonum syndrome. Sagittal T1 image (A) shows the accessory ossicle, os trigonum (arrow). Sagittal PD fat suppressed image (B) demonstrates bone marrow edema involving the os trigonum (short arrow) and the posterior peripheral soft tissue edema with pseudo-joint formation (long arrow).*

FIGURE 11. *Type II Os naviculare. AP radiograph of the foot with the arrow indicating the type II os naviculare creating a psuedo-joint with the navicular bone.*

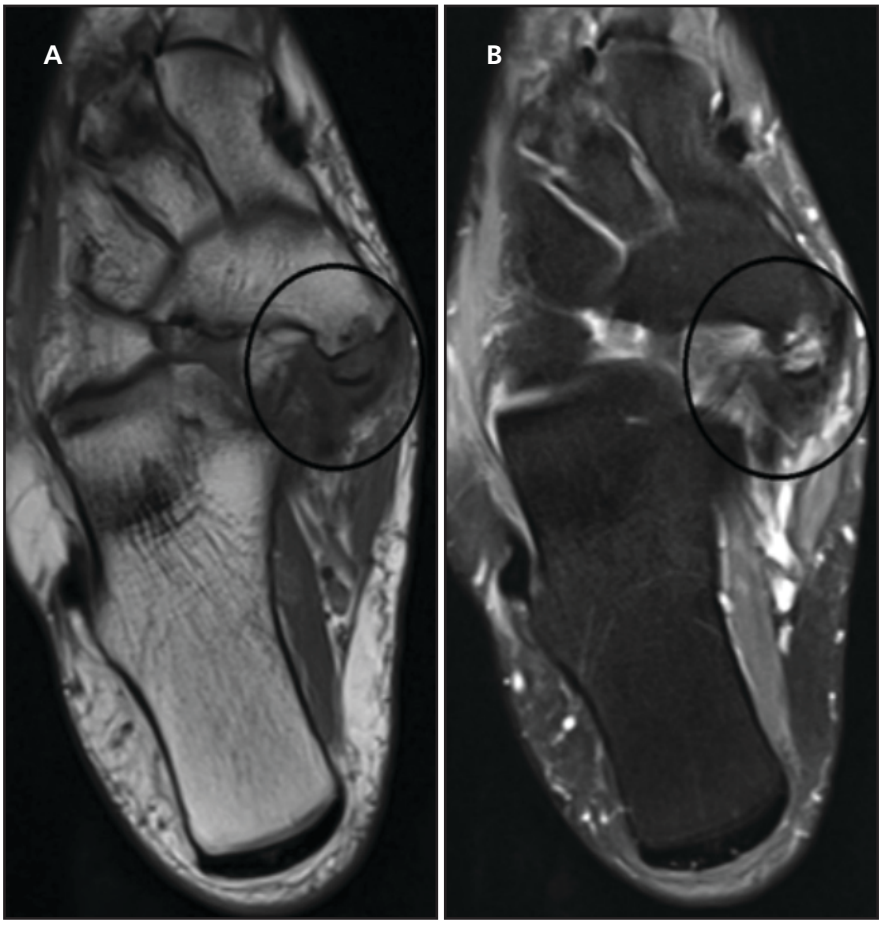

FIGURE 12. *Os naviculare syndrome. T1 (A) and PD fat-suppressed (B) axial images demonstrate os naviculare syndrome. Note the inflammatory changes (hypointense T1 signal and hyperintense PD signal) at the insertion of the posterior tibial tendon (circle). Subchondral cysts are present surrounding the pseudo-joint indicating chronicity in this patient.*

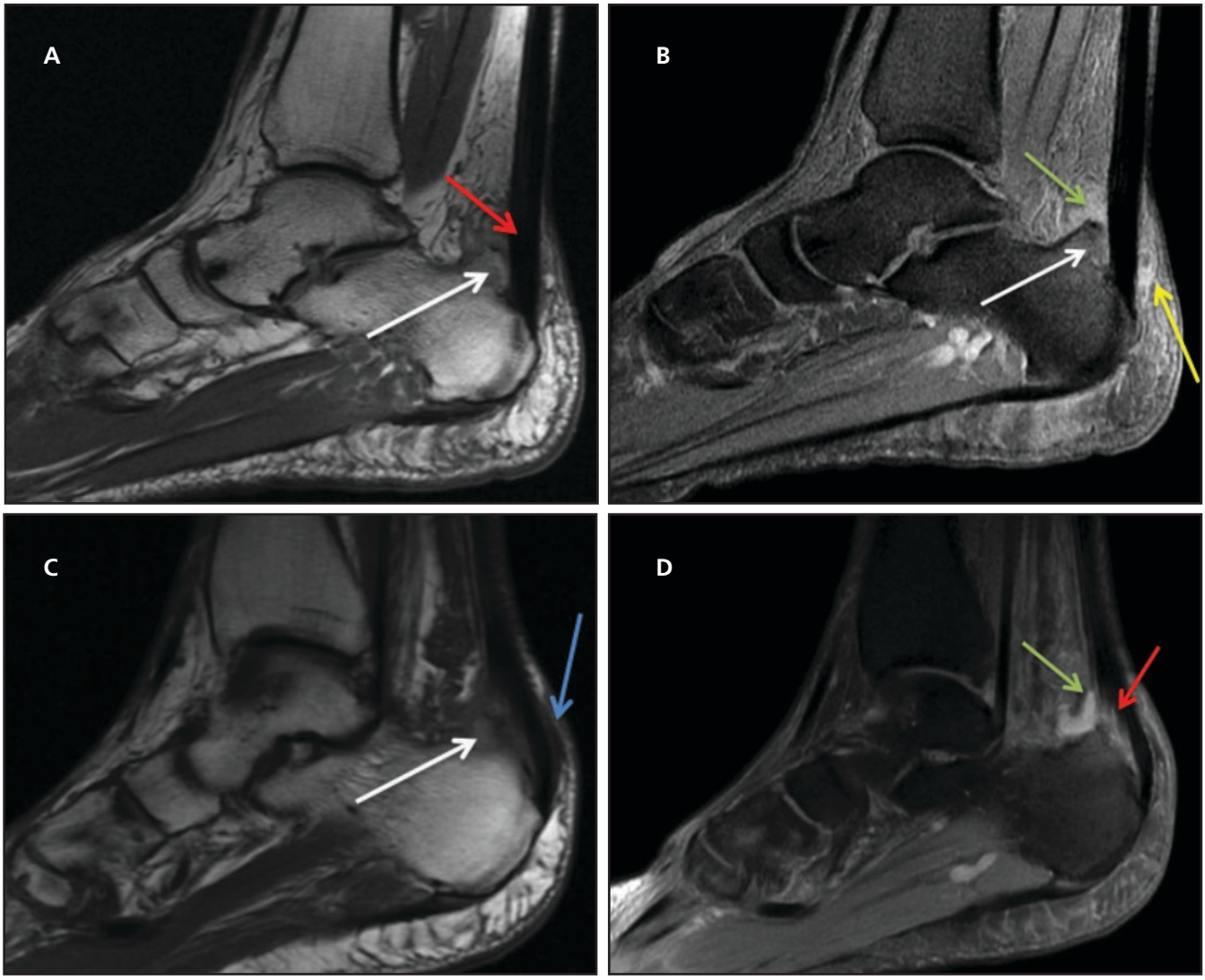

FIGURE 13. *Haglund syndrome in 2 patients. Sagittal T1 image (A) shows a Haglund deformity (white arrow) and intrinsic Achilles tendon signal indicative of tendinosis (red arrow). Sagittal PD FS image (B) demonstrates a Haglund deformity (white arrow), distended retrocalcaneal bursa (green arrow), and retro-Achilles bursitis (yellow arrow). Sagittal T1 image (C) in another patient displays a Haglund deformity (white arrow) and retro-Achilles bursitis (blue arrow). Sagittal PD FS image (D) illustrates a Haglund deformity with reactive marrow changes (white arrow), distended retrocalcaneal bursa (green arrow), and intrinsic Achilles tendon signal, consistent with a partial tear (red arrow).*

of chronic shearing forces at the synchondrosis include inflammation and osteonecrosis.

The MRI findings include bone marrow edema of both the medial pole and posterior aspect of the navicular bone, as well as within the accessory ossicle (**Figure 12**). Destruction of the cartilaginous cap may sometimes be seen as high signal intensity on fat suppressed fluid sensitive sequences. Indirect findings include widening of the ossicle-navicular synchondrosis or fracture of the accessory ossicle. Definitive treatment is surgical intervention, as untreated patients may go on to develop flatfoot, instability, and/or altered gait mechanics.[36,37]

Haglund Syndrome

Haglund syndrome (HS) was first described in 1927 by Patrick Haglund.[38] HS is a chronic overuse syndrome characterized by a chronic inflammatory process with soft tissue irritation or compression by a "Haglund deformity." The Haglund deformity (also known as pump bump or Bauer bump) refers to hypertrophy of the posterior superior calcaneus, which compresses the Achilles tendon between it and footwear. Patients usually present with posterior heel pain that occurs when starting to walk after a period of rest.[38] Haglund syndrome is characterized clinically by painful soft tissue swelling, the so-called "pump bump," at the level of the Achilles tendon insertion.[39] Haglund syndrome is more commonly seen in women secondary to wearing tight fitting footwear, "pumps."[38] Hindfoot varus, low back shoes, and pes cavus are all predisposing factors.[38] The condition results in mechanically induced

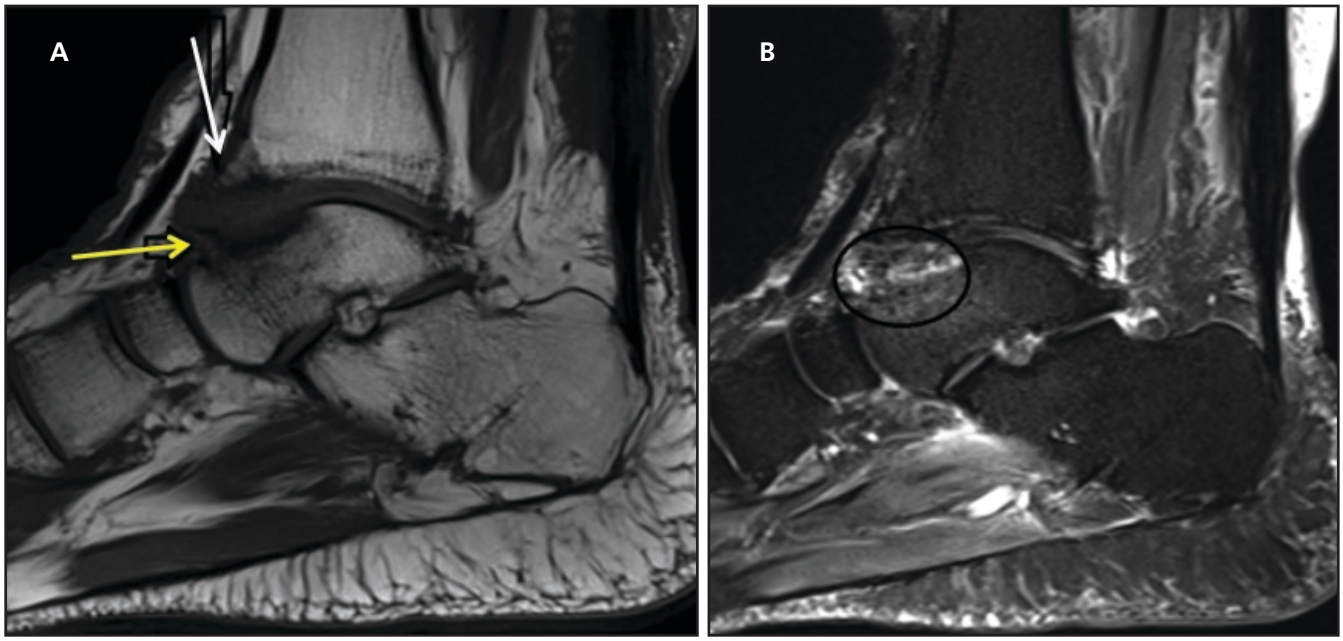

FIGURE 14. *Anterior impingement syndrome. Sagittal T1 weighted image (A) shows "kissing osteophytes" at the anterior tibial plafond (white arrow) and superior talus (yellow arrow) that narrow the tibiotalar angle. Low T1 signal is present within the anterior recess. Corresponding to the low signal within the anterior recess is an inflammatory mass of heterogeneous signal (circle) on the PD fat-suppressed image (B). Peripherally, there is a small joint effusion and bone marrow edema of the talus. Also note there is intrinsic signal with focal thickening of the Achilles, consistent with tendinosis*

inflammation of the superficial bursa, Achilles tendinosis (bump), retrocalcaneal bursitis (bump) due to repetitive compression from the back of the shoes (pumps), and prominent bursal projection of the calcaneus (bump).[38]

On MRI, the diagnosis is most readily made utilizing the sagittal plane. Both T1 and fluid sensitive sequences are useful. The classic triad of findings include retrocalcaneal bursitis, Achilles tendinosis or partial tear, and retro Achilles bursitis (**Figure 13**). Occasionally, bone marrow edema may be seen within the posterior calcaneus involving Haglund's deformity. Treatment for this syndrome is conservative with a combination of nonsteroidal anti-inflammatory drugs (NSAIDs) and steroids. Patients may also respond to a minimally invasive procedure with ultrasound-guided local injection into the retrocalcaneal bursa. Surgical treatment can also be performed with bursectomy and resection of the Haglund deformity.[38]

Anterior Impingement Syndrome

Anterior impingement syndrome (AIS) is a common cause of chronic ankle pain caused by altered joint biomechanics. The classic demographic includes avid soccer players and ballet dancers.[28] These patients usually present with limited and painful dorsiflexion secondary to mechanical impingement by osteophyte formation of the anterior tibial plafond and anterosuperior talus that collide in dorsiflexion, resulting in soft-tissue impingement (**Figure 14A**). Soft-tissue impingement by hypertrophied synovium has also been implicated. As to the cause of the osteophyte formation, many mechanisms have been proposed. The current general consensus is that it is multifactorial.[28] A possible mechanism of injury is repetitive forced dorsiflexion leading to repeated microtrauma, trabecular microfactures, and periosteal hemorrhage with subsequent new bone formation at the site of injury.[28,29] Another postulated mechanism is traction of the anterior capsule during plantar flexion causing avulsion injuries.[28,29]

MRI is particularly useful in detecting bone marrow edema, synovitis, and soft-tissue thickening within the anterior recess (**Figure 14**). MRI can also aid in assessing the degree of cartilage damage.[28,29,40] Other findings on both conventional weight-bearing radiographs and MRI include narrowing of the tibiotalar joint space, anteriomedial tibial and talar osteophytes, and soft tissue swelling of the anterior compartment. Lastly, an anterior tibotalar degree of $< 60^{o}$ may indicate anterior impingement syndrome.[28] Treatment usually begins with conservative management, including physical therapy, limitation of range of motion, and correction of over pronation. If conservative management fails, arthroscopy or open surgery may be performed to remove the osteophytes and soft tissue abnormalities.

Conclusion

There are a myriad of causes of ankle and hindfoot pain with ligamentous injury, tendon injury, and overuse syndromes being among the more common etiologies. It is imperative for the radiologist to have a working knowledge of normal anatomy, anatomic variants that mimic pathology or predispose patients to injury, and the

spectrum of imaging findings of multiple pathological conditions on various modalities. Applying this knowledge when interpreting imaging studies — particularly MRI — will aid the referring clinician in making the most appropriate treatment decisions.

References

1. Chan KW, Ding BC, Mroczek KJ. Acute and chronic lateral ankle instability in the athlete. Bull NYU Hosp Jt Dis 2011; 69(1):17-26.
2. Rosenberg ZS, Beltran J, Bencardino JT. From the RSNA Refresher Courses. Radiological Society of North America. MR imaging of the ankle and foot. RadioGraphics 2000; 20 Spec No:S153-179.
3. Lee MH, Cha JG, Lee YK et al. The bright rim sign on MRI for anterior talofibular ligament injury with arthroscopic correlation. AJR Am J Roentgenol 2012;198:885-890.
4. Manaster, BJ, Disler, DG, May, DA. Musculoskeletal Imaging: The Requisites2nd ed. St. Louis, MO: Elsevier Health; 2002.
5. Tiemstra JD. Update on acute ankle sprains. Am Fam Physician. 2012; 85:1170–1176.
6. Maughan, Karen. Ankle sprain. In: UpToDate, Post TW (Ed.), UpToDate, Waltham, MA, 2014. Accessed December 30, 2014.
7. Nazarenko A, Beltran LS, Bencardino JT. Imaging evaluation of traumatic ligamentous injuries of the ankle and foot. Radiol Clin North Am 2013; 51:455–478.
8. Chhabra A, Subhawong TK, Carrino JA. MR imaging of deltoid ligament pathologic findings and associated impingement syndromes. RadioGraphics 2010; 30(3):751-761.
9. Waterman BR, Belmont PJ, Cameron KL, et al. Risk factors for syndesmotic and medial ankle sprain: role of sex, sport, and level of competition. Am J Sports Med 2011; 39(5):992–998.
10. Cheung, YY. Soft tissue injury to the ankle: ligament injuries. In: Pope T, Bloem HL, Beltran J, Morrison WB, Wilson DJ, eds. Musculoskeletal Imaging. 2nd ed. Philadelphia, PA: Saunders Elsevier; 2015: 455-473.
11. Helms, CA, Major, NM, Anderson, MW, et al. Foot and ankle. In: Musculoskeletal MRI. 2nd ed. Philadelphia, PA: Saunders Elsevier; 2009; 384-429, 50-79.
12. Torbert JT, Doan-Johnson S. OrthopaedicsOne ArticlesIn: OrthopaedicsOne - The Orthopaedic Knowledge NetworkAchilles tendon ruptureCreated Feb 02, 2008. http://www.orthopaedicsone.com/x/LIFF Accessed January 6, 2015.
13. Maffulli N, Sharma P, Luscombe K. Achilles tendinopathy: aetiology and management. J R Soc Med. 2004; 97(10):472-476.
14. Ham P, Maughan, K. Achilles tendinopathy and tendon rupture. In: UpToDate, Post TW (Ed.), UpToDate, Waltham, MA, 2014. Accessed December 30, 2014.
15. Hamilton, W. Flexor Hallicus longus tendinopathy. In: Reider B, Davies G, Provencher M, eds. Orthopaedic Rehabilitation of the Athlete. Philadelphia, PA: Elsevier; 2015; 1492-1510.
16. Irwin, T. Tendon injuries of the foot and ankle. In: Miller, MD, Thompson SR, eds. DeLee & Drez's Orthopedic Sports Medicine, 4th ed. Philadelphia, PA: Saunders Elsevier; 2015; 1408-1427.
17. Coughlin MJ, Schon LC. Disorders of the tendons. In: Coughlin MJ, Saltzman CL, Anderson RB, eds. Mann's Surgery of the Foot and Ankle, 9th ed. Philadelphia: Mosby Saunders Elsevier; 2013;1188-1291.
18. Kadakia, A. Imaging of the foot and ankle. In: Miller, MD, Thompson SR, eds. DeLee & Drez's Orthopedic Sports Medicine, 4th ed. Philadelphia, PA: Saunders Elsevier; 2015; 1331-1342.
19. O'Sullivan E, Carare-NNadi R, et al. Clinical significance of variations in the interconnections between flexor digitorum longus and flexor hallucis longus in the region of the knot of Henry. Clin Anat 2005; 18:121-125.
20. Lo LD, Schweitzer ME, Fan JK, et al. MR imaging findings of entrapment of the flexor hallicus longus tendon. AJR Am J Roentgenol 2001;176(5):1145-1148.
21. Bare AA, Haddad SLTenosynovitis of posterior tibial tendon. Foot Ankle Clin 2001; Mar;6(1):37-66.
22. Schweitzer ME, Karasick D. MR imaging of disorders of the posterior tibialis tendon. AJR Am J Roentgenol September 2000, Volume 175(3).
23. Lee M, Chung CB, Cho JH, et al. Tibialis anterior tendon and extensor retinaculum: imaging in cadavers and patients with tendon tear. AJR Am J Roentgenol 2006; 187(2)161-168.
24. Gallo RA, Kohlman BH, Daffner RDMRI of tibialis anterior tendon rupture. Skeletal Radiol 2004; 33(2)102-106.
25. Sammarco JV, Sammarco GJ, Henning C, et al. J Surgical repair of acute and chronic tibialis anterior tendon ruptures. Bone Joint Surg Am 2009; 91(2):325-332.
26. Tol JL, Slim E, van Soest AJ, van Dijk CN. The relationship of the kicking action in soccer and anterior ankle impingement syndrome: a biomechanical analysis. Am J Sports Med 2002; 30:45-50.
27. Marotta JJ, Micheli LJ. Os trigonum impingement in dancers. Am J Sports Med 1992; 20(5):533-536.
28. Donovan A, Rosenberg ZS. MRI of ankle and lateral hindfoot impingement syndromes. AJR Am J Roentgenol 2010; 195(3):595-604.
29. Cerezal L, Abascal F, Canga A, et al. MR imaging of ankle impingement syndromes. AJR Am J Roentgenol 2003; 181(2):551-559.
30. Robinson P, White LM. Soft-tissue and osseous impingement syndromes of the ankle: role of imaging in diagnosis and management. RadioGraphics 2002; 22(6):1457-1469.
31. Bureau NJ, Cardinal E, Hobden R, et al. Posterior ankle impingement syndrome: MR imaging findings in seven patients. Radiology 2000; 215(2):497-503.
32. Karasick D, Schweitzer ME. The os trigonum syndrome: imaging features. AJR Am J Roentgenol 1996; 166(1):125-129.
33. Rosenberg ZS, Cheung YY, Beltran J, et al. Posterior intermalleolar ligament of the ankle: normal anatomy and MR imaging features. AJR Am J Roentgenol 1995; 165(2):387-390.
34. Hedrick MR, McBryde AM. Posterior ankle impingement. Foot Ankle Int 1994; 15(1):2-8.
35. Choi YS, Lee KT, Kang HS et al. MR imaging findings of painful type II accessory navicular bone: correlation with surgical and pathologic studies. Korean J Radiol 2004; 5(4):274–279.
36. Miller TT, Staron RB, Feldman F, et al. The symptomatic accessory tarsal navicular bone: assessment with MR imaging. Radiology 1995; 195(3): 849-853.
37. Birrer RB, Griesemer B, Cataletto MB. Pediatric Sports Medicine for Primary Care. Philadelphia: Lippincott Williams & Wilkins. (2002).
38. Hung EHY, Kowk WK, Tong MMP, et al. Haglund syndrome – a characteristic cause of posterior heel pain. J HK Coll Radiol 2009; 11:183-185.
39. Pavlov H, Heneghan MA, Hersh A et al. The Haglund syndrome: initial and differential diagnosis. Radiology 1982; 144(1):83-88.
40. Umans H. Ankle impingement syndromes. Semin Musculoskelet Radiol 2002; 6(2):133-139.

Neuroimaging Manifestations of NF1 — A Pictorial Review

William T. O'Brien, Sr., D.O.

Department of Radiology, David Grant USAF Medical Center, Travis AFB, CA
Department of Radiology, University of California, Davis School of Medicine, Sacramento, CA

Background

Neurocutaneous syndromes encompass a group of disorders that affect the embryonic ectodermal plate, which includes the central and peripheral nervous systems, as well as the overlying skin. Mesodermal and endodermal structures may be involved, depending on the type and severity of the specific neurocutaneous system. Common developmental abnormalities include dysplasias and often an increased incidence of neoplasms.

Neurofibromatosis type 1 (NF1), also known as von Recklinghausen disease, is the most common of the neurocutaneous syndromes with an incidence of approximately 1 in 2,600 to 1 in 3,500 live births.[1-3] Men and women are affected equally. NF1 is inherited in an autosomal dominant fashion with variable pathological and clinical expression. Approximately half of all cases result from spontaneous mutations of the NF1 gene.[4] The genetic defect affects chromosome 17q12 and results in decreased production of neurofibromin, which acts as a tumor suppressor. The disease affects the brain, skull, orbits, spine, musculoskeletal system, and skin/integumentary system, although there is significant variability in the type and severity of clinical manifestations.[3] Diagnostic criteria for NF1 include the presence of 2 or more of the following: first degree relative with NF1, 6 or more café-au-lait spots, 2 or more neurofibromas (NFs) or 1 plexiform neurofibroma (PNF), optic pathway glioma, bony dysplasia, axillary or inguinal freckling, and 2 or more Lisch nodules.[5,6] Central nervous system (CNS) abnormalities occur in approximately 15%-20% of NF1 patients.[7]

Intracranial Manifestations of NF1

Parenchymal Involvement and Neoplasias

Intracranial CNS manifestations include characteristic NF1 "spots" and low-grade neoplasms. The NF1 "spots" are regions of signal abnormality involving the basal ganglia, thalami, dentate nuclei, cerebellar peduncles, optic radiations, and brainstem in children and adolescents; they are thought to represent regions of myelin vacuolization **(Figure 1)**. They are hyperintense on T2 sequences and typically iso- to mildly hyperintense on T1 images. There should be no mass effect or enhancement, as enhancement or significant mass effect suggests development of a low-grade glioma. The lesions may wax and wane for the first decade of life or so and then regress.[8] They are uncommon after the second decade of life.

The most common CNS neoplasm associated with NF1 is a low-grade optic pathway glioma (OPG). The majority of children with OPGs have NF1,[9,10] while approximately 20% of patients with NF1 have OPGs.[11,12] The presence of bilateral optic nerve gliomas is considered pathognomonic for NF1. The tumors cause enlargement, elongation and "buckling" of the optic nerve, resulting in the "dotted i" appearance on axial images **(Figure 2)**. Enlargement and benign bony remodeling of the optic canal may also be seen. Although low-grade, the lesions may extend to the optic chiasm, and along the optic tracts and radiations **(Figure 3)**. Visual loss and interval change in size are the most important considerations in terms of managing OPGs. The tumors are hypointense on T1 and hyperintense on T2 sequences. Expansion of CSF within the optic nerve sheath complex may be seen, possibly due to CSF trapping. Enhancement characteristics are variable, especially in the

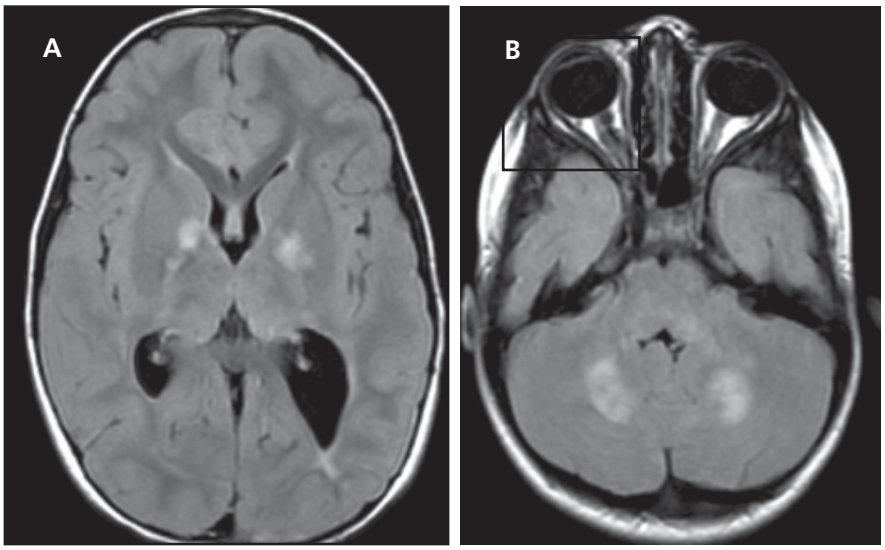

FIGURE 1. *NF1 "spots." Axial fluid-attenuated inversion recovery (FLAIR) images demonstrate multiple foci of increased signal intensity without mass effect involving the basal ganglia and deep white matter tracts (A), as well as the cerebellum (including dentate nuclei) and the brainstem (B).*

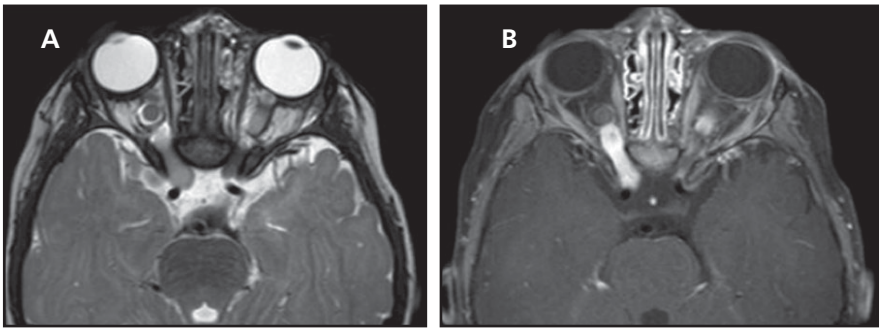

FIGURE 2. *Optic pathway glioma. Axial T2 image (A) demonstrates enlargement and buckling of the bilateral prechiasmatic and intraorbital segments of the optic nerves, resulting in the "dotted i" appearance. There is also increased CSF signal intensity within the right optic nerve-sheath complex. Axial T1 postcontrast image with fat suppression (B) reveals abnormal enhancement of the enlarged optic nerves. Reprinted with permissions: O'Brien WT.* Top 3 Differentials in Neuroradiology. *New York: Thieme, 2015.*

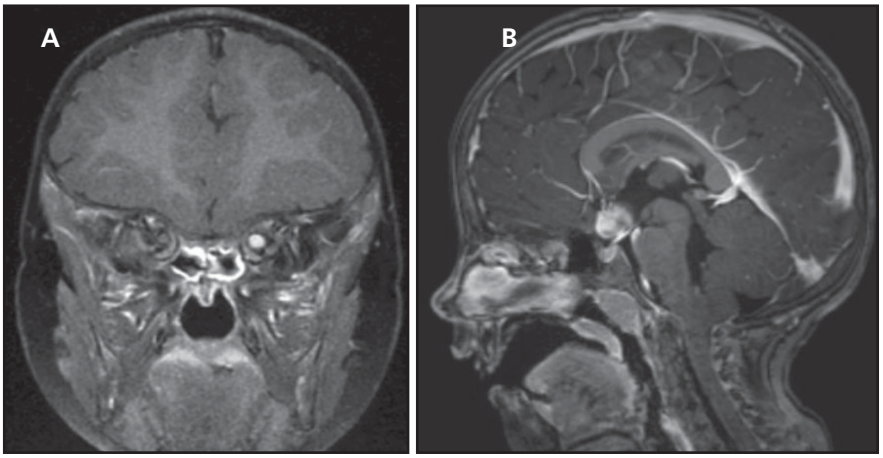

FIGURE 3. *Optic pathway glioma. Coronal T1 postcontrast image with fat suppression (A) shows abnormal enlargement and enhancement of the intraorbital left optic nerve. Sagittal T1 postcontrast image with fat suppression in a different patient (B) reveals an enhancing suprasellar mass centered within the optic chiasm.*

setting of ongoing treatment, and are less reliable in terms of directing treatment decisions compared to a change in tumor size or extent. Treatment options include chemotherapy, surgery, and radiation therapy, although radiation therapy is generally avoided in patients with NF1.[13]

Low-grade cerebellar, brainstem, tectal plate, and basal ganglia gliomas are also common and have an increased incidence in the setting of NF1; the vast majority are pilocytic astrocytomas, although high-grade gliomas may occasionally be seen as well. Pilocytic variants involving the posterior fossa, brainstem, and optic pathways commonly present as cystic tumors with an enhancing mural nodule **(Figures 4 and 5)**. Enhancement may be seen along the cyst wall as well, which often indicates tumor cells lining the cystic component **(Figure 5)**.[14] On MRI, tectal plate gliomas are typically T2 hyperintense and iso- to hypointense on T1 with no or minimal enhancement **(Figure 6)**. More aggressive gliomas most often present in the pons and appear as ill-defined, infiltrative masses with variable enhancement patterns. Higher-grade components demonstrate central necrosis with increased peripheral enhancement and perfusion, as well as restricted diffusion.[14] Obstructive hydrocephalus may result from mass effect associated with tectal plate, cerebellar, or brainstem gliomas or as a result of aqueductal stenosis, which has an increased incidence in patients with NF1.

Orbital Involvement

In addition to OPGs (described above), orbital findings include sphenoid wing dysplasia with associated pulsatile exophthalmos, buphthalmos (globe enlargement), and intraorbital extension of a plexiform neurofibroma. Sphenoid wing dysplasia is a characteristic finding of NF1 but is relatively uncommon. The greater wing of the sphenoid is most often involved. Although the precise etiology of sphenoid wing dysplasia is not entirely understood, recent studies suggest that the

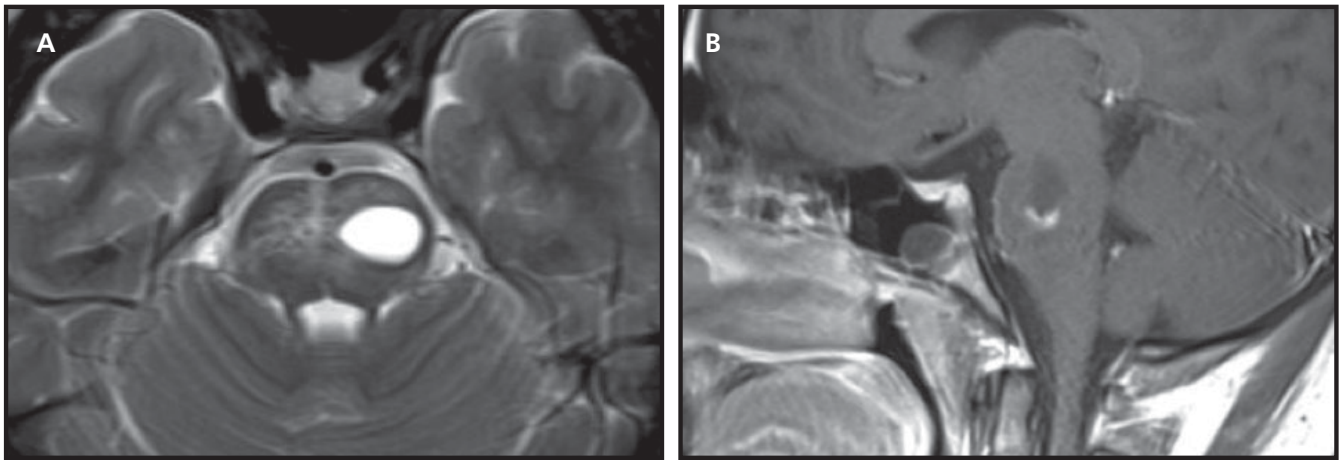

FIGURE 4. *Brainstem juvenile pilocystic astrocytoma. Axial T2 image through the pons (A) reveals a cystic lesion to the left of midline with mild mass effect and surrounding edema. Sagittal T1 postcontrast image (B) shows a nodular enhancing component along the inferior margin of the mass.*

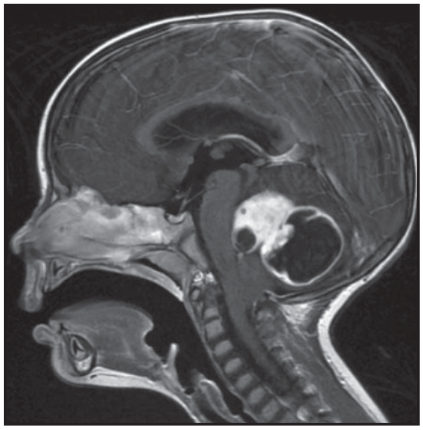

FIGURE 5. *Posterior fossa juvenile pilocytic astrocytoma. Sagittal T1 postcontrast image demonstrates a large cystic and solid posterior fossa mass with an enhancing nodular component along its anterosuperior margin, as well as enhancement along the wall of the cystic component. There is compression of the 4th ventricle and brainstem with obstructive hydrocephalus and inferior displacement of the cerebellar tonsils through the foramen magnum.*

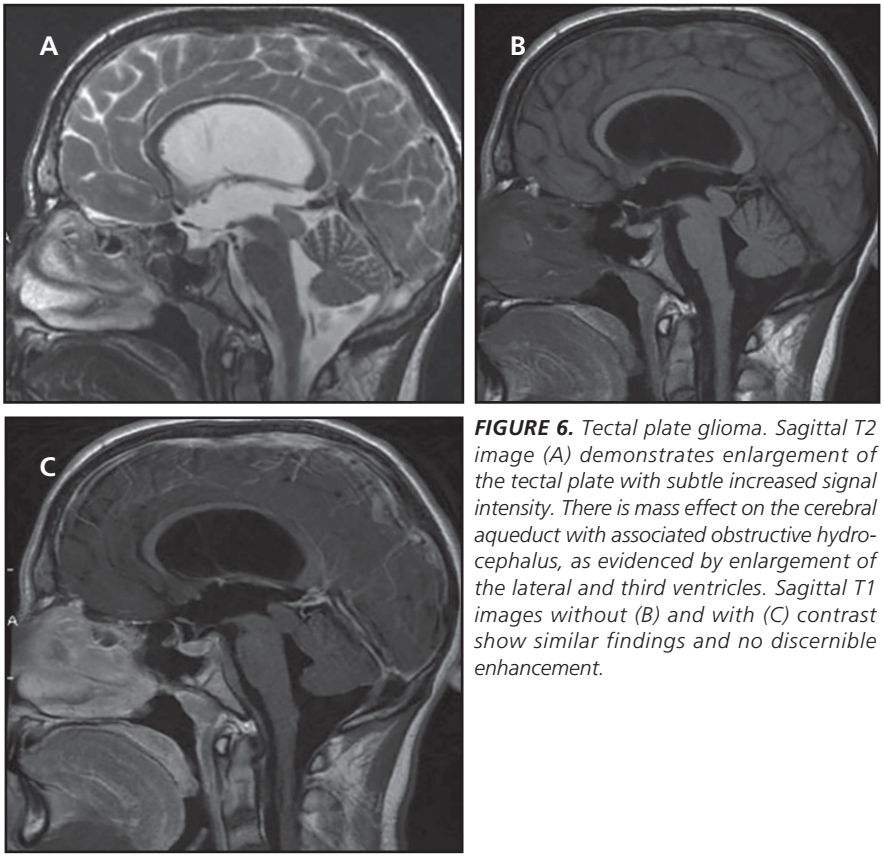

FIGURE 6. *Tectal plate glioma. Sagittal T2 image (A) demonstrates enlargement of the tectal plate with subtle increased signal intensity. There is mass effect on the cerebral aqueduct with associated obstructive hydrocephalus, as evidenced by enlargement of the lateral and third ventricles. Sagittal T1 images without (B) and with (C) contrast show similar findings and no discernible enhancement.*

process may be multifactorial with a combination of bony dysplasia, as well as an ipsilateral plexiform neurofibroma affecting growth and closure of skull base sutures.[15] Cross-sectional imaging demonstrates anterior displacement and thinning of the sphenoid bone with enlargement of the middle cranial fossa in the anteroposterior dimension **(Figure 7)**. Herniation of portions of the temporal lobe and overlying CSF into the posterior margin of the orbit results in pulsatile exophthalmos. Globe enlargement – buphthalmos – may also be seen in the setting of NF1 **(Figure 8)**.

As the name would imply, neurofibromas (NFs) are common in the setting of NF1. NFs are classified as benign peripheral nerve sheath tumors with subcategories, including localized, discrete superficial or deep NFs and diffuse plexiform neurofibromas (PNFs). NFs most often involve the orbits, head and neck, spine, and paraspinal soft tissues in patients with NF1. On MRI, they are hyperintense on T2 and hypointense on T1 sequences with heterogeneous enhancement. Compared to schwannomas, NFs are more likely to demonstrate the target appearance with central decreased and peripheral increased T2 signal intensity.[16]

PNFs refer to a network of nerve fascicles and thickened fibers that occur along the longitudinal axis of peripheral

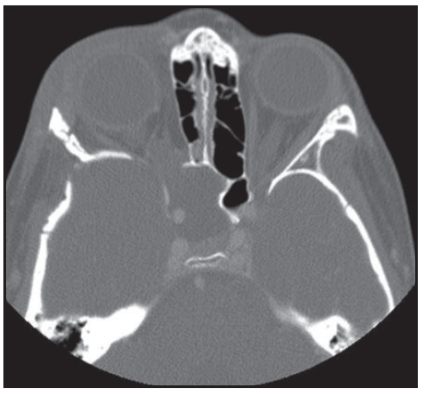

FIGURE 7. *Sphenoid wing dysplasia. Axial CT image in bone window reveals anterior displacement and thinning of the sphenoid bone on the right with enlargement of the middle cranial fossa in the anteroposterior dimension. A soft tissue mass extending through and expanding the right optic canal, consistent with an optic pathway glioma, is partially seen.*

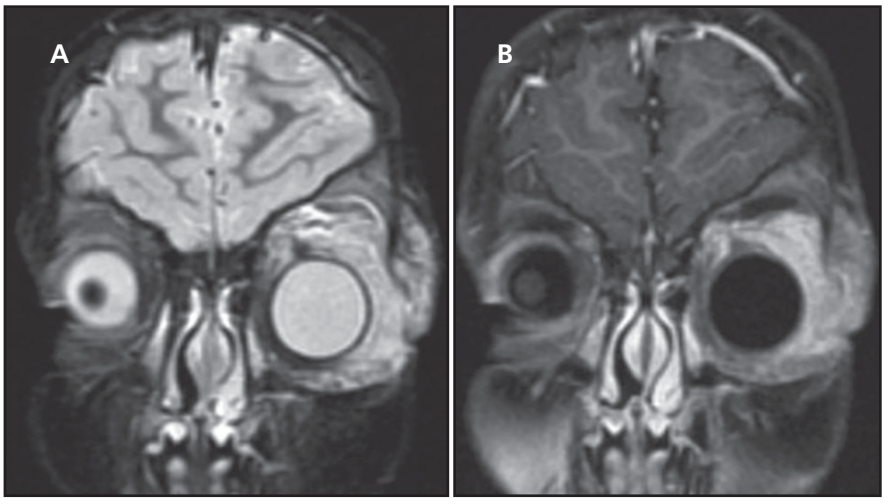

FIGURE 9. *Plexiform neurofibroma. Coronal fluid-sensitive T2 (A) and postcontrast T1 (B) images with fat suppression (A) demonstrate a large enhancing T2 hyperintense mass with intermediate to hypointense linear striations involving the pre- and postseptal compartments of the left orbit, as well as involvement of the suprazygomatic masticator space on the left. There is mass effect on the left with proptosis.*

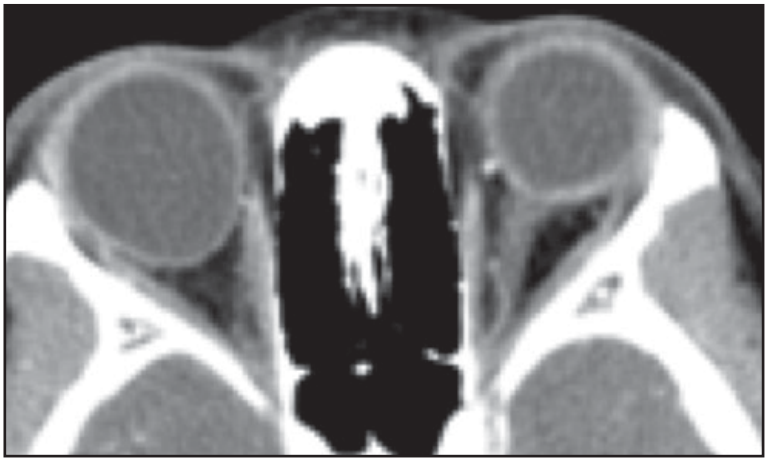

FIGURE 8. *Buphthalmos. Axial CT image reveals enlargement of the right globe in a young child with NF1, consistent with buphthalmos.*

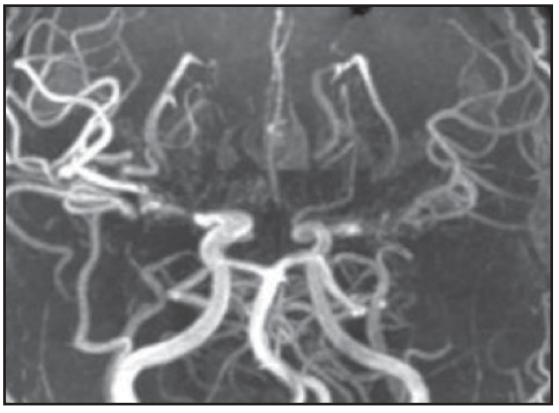

FIGURE 10. *Vasculopathy/moya moya. Reformatted image from an MR angiogram demonstrates occlusion of the terminal carotid and proximal cerebral arteries with multiple basilar and meningeal collateral vessels, consistent with moya moya.*

nerves. They appear more infiltrative on MRI with T2 hypointense septations and heterogeneous enhancement **(Figure 9)**. PNFs commonly involve the orbit, skull base, and spine. PNFs are clinically important, since approximately 10% will undergo malignant degeneration.[17]

Vascular Involvement

NF1 is known to affect the intracranial vasculature; however, the incidence of vascular abnormalities is relatively low. The most common vascular abnormalities include regions of stenosis or occlusion, often resulting in secondary moya moya disease. Additional vascular abnormalities include arteriovenous malformations and fistulae, dolichoectasia, as well as an increased incidence of aneurysms.[18]

Moya moya is characterized by progressive occlusion of the supraclinoid internal carotid artery and/or proximal cerebral arteries with development and enlargement of multiple basilar collateral vessels. The term "moya moya" means "puff of smoke" in Japanese and corresponds to the appearance of abnormal collateral vessels depicted on angiography when the entity was first described.[19] On MR angiography, there is loss of flow signal intensity at the carotid terminus and/or proximal cerebral arteries with multiple enlarged basilar collateral vessels, which have a smudgy appearance **(Figure 10)**. This results in the characteristic "puff of smoke" appearance. Patients are at risk of ischemia and subsequent infarcts, especially in a watershed distribution, as well as hemorrhage. Perfusion imaging can be used to monitor disease progression and determine whether or not there is an adequate vascular reserve.

Spinal Manifestations of NF1

Spinal manifestations of NF1 include multiple bilateral intraspinal and paraspinal neurofibromas. Spinal lesions may

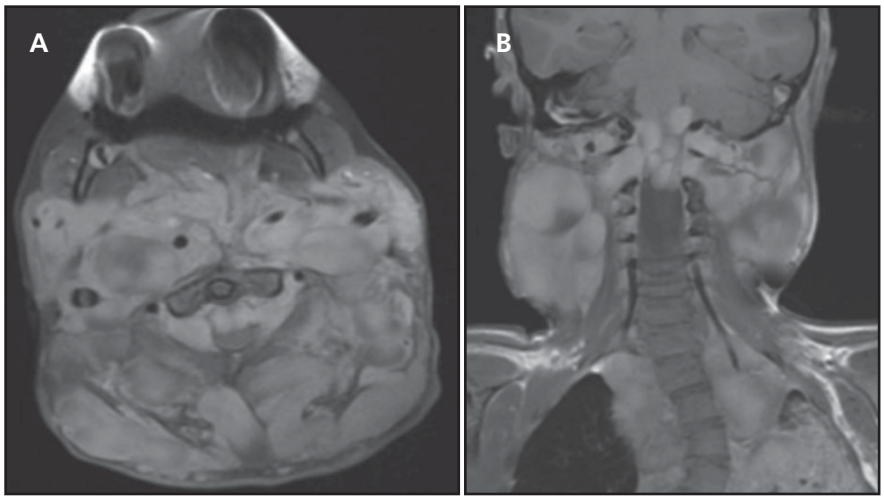

FIGURE 11. *Spinal (plexiform) neurofibromas. Axial (A) and coronal (B) T1 postcontrast images with fat suppression reveal multiple, large, lobulated, enhancing paraspinal, extradural, and intradural extramedullary masses. Cord compression is seen at the cervicomedullary junction. The coronal image (B) shows focal scoliosis within the upper thoracic spine associated with numerous paraspinal masses, as well as foraminal extension and expansion within the upper cervical spine. There is partial collapse of the left upper lobe.*

FIGURE 12. *Malignant peripheral nerve sheath tumor. Coronal T2 image demonstrates a large dumbbell-shaped mass extending through and expanding a neural foramen within the lumbar spine on the left. The superior portion of the intraspinal component is ill-defined and increased in size from comparison examination. Multiple NFs are seen at adjacent levels.*

FIGURE 13*. Kyphoscoliosis. Sagittal T1 image with fat suppression reveals bony dysplasia of the mid-lower cervical spine with a focal kyphotic gibbus deformity. There is underlying cord compression at the apex of the bony deformity, as well as abnormal enhancement within the epidural and paraspinal soft tissues, consistent with NFs.*

be intradural, intradural and extradural, or purely extradural. On imaging, smaller lesions are often T2 hyperintense with prominent enhancement, similar to schwannomas. Larger lesions are more heterogeneous in signal intensity and enhancement patterns. As with NFs elsewhere and as discussed above, neurofibromas are more likely than schwannomas to demonstrate the "target sign," which refers to peripheral increased and central decreased T2 signal intensity. Intra- and extradural lesions extend through and expand the bony neural foramina with benign bony remodeling **(Figure 11)**.

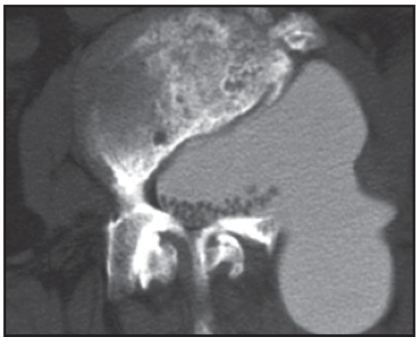

FIGURE 14. *Lateral thoracic meningocele. Axial image from a CT myelogram demonstrates a large meningocele extending through and expanding the left neural foramen and into the adjacent paraspinal soft tissues. Image courtesy of Paul M. Sherman, M.D.*

Although the majority of cases of malignant peripheral nerve sheath tumors occur in the setting of neurofibromatosis, the estimated incidence of malignant peripheral nerve sheath tumors in NF1 patients is approximately 5%.[20] Malignant lesions tend to be larger, more ill-defined and heterogeneous, and grow fairly rapidly with regions of central necrosis **(Figure 12)**. Large retroperitoneal PNFs may be present and are prone to malignant degeneration, which is best characterized by interval growth on subsequent imaging.

Additional spinal manifestations include kyphoscoliosis **(Figure 13)**, dural ectasia with posterior vertebral body scalloping, and lateral thoracic meningoceles. The bony manifestations of NF1 may be due to a primary bony dysplasia and/or bony changes associated with adjacent neurofibromas.[21] Lateral thoracic meningoceles are thought to result from dural ectasia/meningeal dysplasia **(Figure 14)**.

Extra-CNS Manifestations of NF1

Extra CNS and spinal manifestation are beyond the scope of this review, but include cutaneous abnormalities, such as cutaneous neurofibromas and café-au-lait spots; pseudoarthroses and bowing deformities affecting the long bones of the extremities; "ribbon" ribs;

and overgrowth or hypertrophy of all or a portion of a limb. NF1 is associated with an increased incidence of neoplasia, to include pheochromocytoma, gastrointestinal stromal tumors, leukemia, and lymphoma.

Conclusion

Neurofibromatosis type 1 is the most common of the neurocutaneous syndromes, affecting multiple sites and organ systems. CNS manifestations occur in roughly 10%-20% of patients and include regions of myelin vacuolization (NF1 "spots"); multiple tumors, to include gliomas (optic pathway and spinal are the most common) and variants of neurofibromas; bony dysplasia; vascular abnormalities; and dural ectasia. Understanding the characteristic imaging findings, as well as their clinical significance and expected evolution, is critical in correctly interpreting neuroimaging studies in this patient population, and appropriately guiding management decisions.

References

1. Lammert M, Friedman JM, Kluwe L, et al. Prevalence of neurofibromatosis 1 in German children at elementary school enrollment. Arch Dermatol 2005; 141(1): 71-74.
2. Evans DG, Howard E, Giblin C, et al. Birth incidence and prevalence of tumor-prone syndromes: estimates from a UK family genetic register service. Am J Genet A 2010; 152A(2):327-332.
3. Jett K, Friedman JM. Clinical and genetic aspects of neurofibromatosis 1. Genet Med 2010 12(1):1-11.
4. Tonsgard JH. Clinical manifestations and management of neurofibromatosis type 1. Semin Pedatr Neurol 2006; 13:2-7.
5. Williams VC, Lucas J, Babcock MA, et al. Neurofibromatosis type 1 revisited. Pediatrics 2009; 123: 124 -133.
6. Ferner RE, Huson SM, Thomas N, et al. Guidelines for the diagnosis and management of individuals with neurofibromatosis 1 (NF1). J Med Genet 2007; 44: 81-88.
7. Braffman B, Naidich TP. The phakomatoses, part 1: neurofibromatosis and tuberous sclerosis. Neuroimaging Clin North Am 1994; 4:299-324.
8. Sevick R, Barkovich A, Edwards M, et al. Evolution of white matter lesions in neurofibromatosis type 1: MR findings. Am J Roentgenol 1992; 159:171-175.
9. Kornreich L, Blaser S, Schwarz M, et al. Optic pathway glioma: correlation of imaging findings with the presence of neurofibromatosis. Am J Neuroradiol 2001; 22:1963-1969.
10. Nicolin G, Parkin P, Mabbott D, et al. Natural history and outcome of optic pathway gliomas in children. Pediatr Blood Cancer 2009; 53:1231-1237.
11. Listernick R, Charrow J, Greenwald M, et al. Natural history of optic pathway tumors in children with neurofibromatosis type 1: a longitudinal study. J Pediatr 1994 ;125:63-66.
12. Blazo MA, Lewis RA, Chintagumpala MM, et al. Outcomes of systematic screening for optic pathway tumors in children with neurofibromatosis type 1. Am J Med Genet 2004; 127:224-229.
13. Avery RA, Fisher MJ, Liu GT. Optic pathway gliomas. J Neuro-Ophthalmol 2011; 31:269-278.
14. O'Brien WT. Imaging of primary posterior fossa brain tumors in children. J Am Osteopath Coll Radiol 2013; 2(3):2-12.
15. Jacquemin C, Bosley TM, Liu D, et al. Reassessment of sphenoid dysplasia associated with neurofibromatosis type 1. Am J Neuroradiol 2002; 23:644-648.
16. Carra BJ, Sherman PM. Intradural spinal neoplasms: a case based review. J Am Osteopath Coll Radiol 2013 2(3):13-21.
17. Evans DG, Baser ME, McGaughran J, et al. Malignant peripheral nerve sheath tumours in neurofibromatosis 1. J Med Genet 2002; 39(5): 311-314.
18. Rodriguez D, Poussaint TY. Neuroimaging findings in neurofibromatosis type 1 and 2. Neuroimag Clin N Am 2004; 14:149-170.
19. Burke GM, Burke AM, Sherma AK, et al. Moyamoya disease: a summar. Neurosurg Focus 2009; 26(4): 1-10.
20. Lin J, Martel W. Cross-sectional imaging of peripheral nerve sheath tumors: characteristic signs on CT, MR imaging, and sonography. Am J Roentgenol 2001; 176:75-82.
21. Sher BJ, Duncan IC. Neurofibromatosis type 1 – some cranial and spinal manifestations. SA J Radiol 2004; 8(3):32-35.

The views expressed in this material are those of the author, and do not reflect the official policy or position of the U.S. Government, the Department of Defense, or the Department of the Air Force.

Temporal Lobe Signal Abnormality

Michael E. Zapadka, D.O.

Department of Radiology, Wake Forest Baptist Health, Winston-Salem, NC

Case Presentation

An 18-year-old man presented to the emergency department following a witnessed seizure with altered mental status. Clinical exam was limited due to patient's status. An MRI was performed **(Figure 1)**.

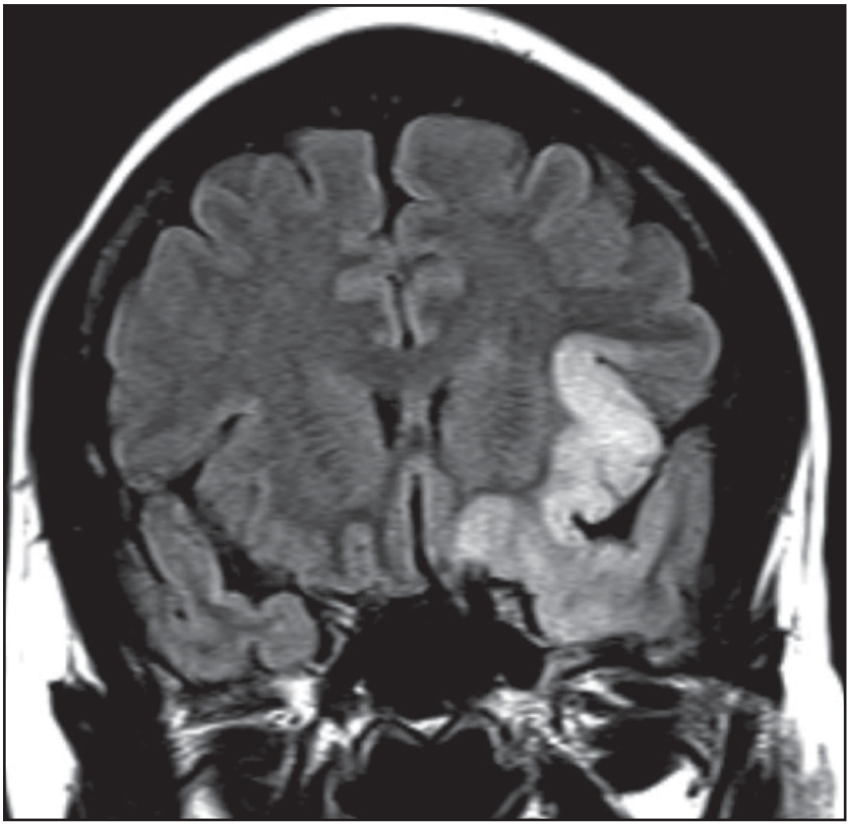

FIGURE 1. *Coronal FLAIR (fluid-attenuated inversion recovery) image demonstrates abnormal hyperintense signal and gyral swelling involving the left insula, mesial temporal lobe, and inferior frontal lobe.*

Key Imaging Finding(s)

Temporal lobe cortically based edema

Differential Diagnosis Based on FLAIR Finding

Encephalitis (HSV, autoimmune)
Gliomatosis cerebri
Peri- or postictal edema
Infarction

Additional Key Images and Findings in (Figure 2)

Discussion

The differential diagnosis in a patient with cortically-based temporal lobe signal abnormality on MRI is broad and includes etiologies such as infection, tumor, and ischemia, among other pathological processes. Unfortunately, the imaging findings are often nonspecific with overlapping appearances. When imaging is correlated with certain key clinical features, however, the radiologist can often make an immediate and profound impact on patient care. This case discussion will highlight important entities with a predilection for the temporal lobes and limbic system.

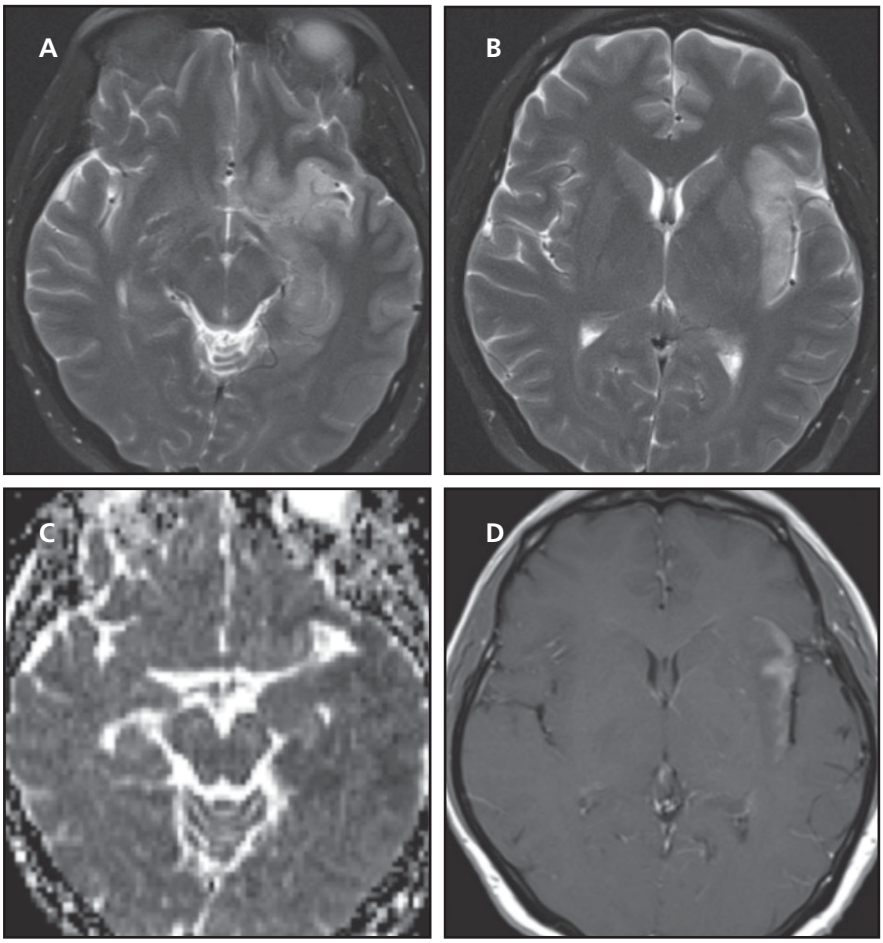

FIGURE 2. *Axial T2 (A and B) images demonstrate abnormal T2 hyperintensity predominantly involving the cortex of the left inferior frontal lobe, mesial temporal lobe, and insula with areas of subtle restricted diffusion on ADC (dark signal, C). Axial postcontrast T1 image (D) shows enhancement along the insular cortex.*

Encephalitis

Herpes simplex encephalitis (HSE)

Multiple subtypes of the herpes virus family are neurotropic and may cause devastating neurologic injury. Herpes simplex virus (HSV) 1 is ubiquitous and generally acquired during childhood, typically affecting the skin and facial mucosa (i.e., cold sores). HSV 2 is another common subtype that is usually acquired through sexual contact with individuals that may or may not have exhibited active genital lesions. It is important to note that neonatal HSE is most often caused by vertical transmission of HSV 2 from an infected vaginal canal during delivery. Both the clinical and imaging manifestations of HSV 2 will differ from reactivated HSV 1, the latter of which is the focus of this discussion. It is essential for radiologists to be familiar with the imaging manifestations of HSV 1, as it is the most common cause for fatal sporadic viral encephalitis in the U.S.[1]

Herpes simplex encephalitis (HSE) may ensue during the primary phase of HSV infection, but the majority of encephalitis cases occur due to reactivation of latent HSV 1 virus. The virus initially gains entry into the CNS via the nasopharyngeal mucosa with retrograde dissemination along trigeminal nerve branches to the trigeminal ganglion, where it is harbored in a latent fashion. Viral reactivation may be spontaneous or secondary to various stressors, to include trauma, immunosuppression, or hormonal fluctuations.[2]

HSE has no gender predilection and may occur at any age but does follow a bimodal age distribution with one-half of cases affecting those less than 20 years of age and the other half in those greater than 50 years of age. Patients usually present with a viral prodrome including fever and headache that may progress to seizures, behavioral changes, hallucinations, and altered mental status. Despite antiviral therapy, HSE remains a devastating infection with mortality rates as high as 70%. Most survivors will have permanent neurologic sequelae. When HSE is suspected clinically or by imaging, presumptive antiviral therapy should be instituted urgently due to its high morbidity and mortality; however, polymerase chain reaction (PCR) is necessary for definitive diagnosis.

The imaging findings are nonspecific, but HSE characteristically involves the limbic system to varying degrees. The anterior and medial temporal lobes, insula, subfrontal region, and cingulate gyri are most often affected and are frequently bilateral and asymmetric.[2] While medial temporal

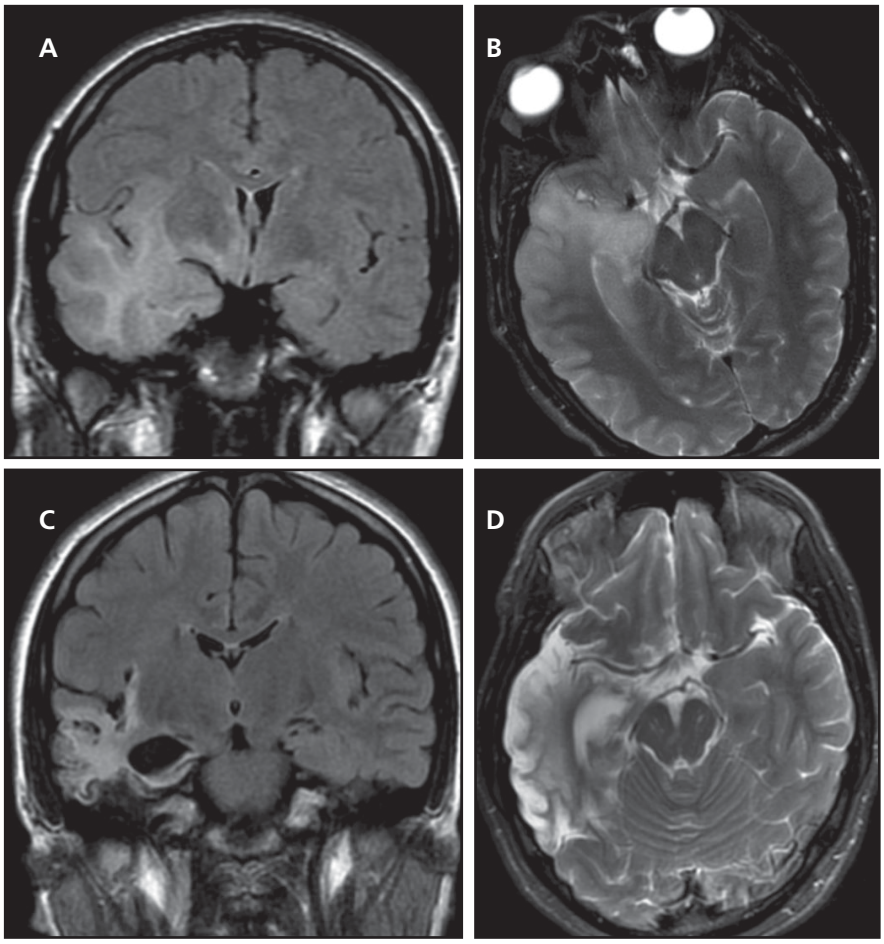

FIGURE 3. *Herpes simplex encephalitis (HSE). Coronal FLAIR (A) and axial T2 (B) images demonstrate abnormal hyperintense signal involving the right insula, temporal lobe, and inferomedial frontal lobe with associated mass effect. Repeat coronal FLAIR (C) and axial T2 (D) images 4 months later following treatment with acyclovir demonstrates corresponding areas of encephalomalacia and gliosis with parenchymal volume loss, reflecting the chronic sequelae of HSE.*

lobe abnormality often prompts the radiologist to suggest HSE, it is important to remember that any portion of the limbic system may be involved in isolation.

Noncontrast CT may be normal in the early stage of HSE, or an abnormality may be very difficult to detect, in part due to beam-hardening artifact obscuring the medial temporal lobes. However, recognizing edema or mass effect involving the medial temporal lobe, insula, or other portions of the limbic system should prompt the radiologist to specifically suggest HSE in the differential diagnosis. It is also imperative to directly communicate as much with the referring clinician, since prompt diagnosis and treatment are critical to preventing severe neurologic sequelae.

MRI is the modality of choice when HSE is suspected. Restricted diffusion along the cortex of the limbic structures may be the earliest finding detected. Cortical and subcortical T2 and FLAIR hyperintensity with indistinctness at the gray-white interface are also typical findings. Early in HSE, there is often relative sparing of the white matter, but more extensive edema will develop as HSE progresses. T1-weighted imaging shows gyral swelling, but the T1 signal changes are usually less dramatic than on T2 or FLAIR. In the subacute stages of HSE, gyriform T1 hyperintensity or susceptibility on gradient echo (GRE) or susceptibility weighted imaging (SWI) sequences reflects petechial hemorrhage. Gyriform or patchy enhancement may also be seen at this stage secondary to blood-brain barrier breakdown. In chronic stages, encephalomalacia and gliosis develop **(Figure 3)** with gyriform T1 hyperintensity indicating cortical laminar necrosis. Generally the basal ganglia are spared; brainstem involvement is rare. The distribution of findings in children with HSE may differ and include extratemporal, extralimbic involvement, most often affecting the parietal cortex.[2]

Autoimmune encephalitis

Multiple forms of autoimmune encephalitis have been described, which may or may not be associated with a systemic malignancy. Among the autoimmune encephalitides, paraneoplastic limbic encephalitis (PLE) is most commonly implicated. PLE results from immune mediated mechanisms with antineuronal antibodies often detected in serum or CSF, but without any direct or metastatic tumor invasion of the brain. Overall, PLE is relatively rare and affects less than 1% of patients with systemic cancer, most commonly small cell lung cancer, followed by testicular and breast cancer.[2]

Neurologic symptoms of PLE may be the initial manifestation of a systemic malignancy; therefore, recognition of this entity is key to pursuing extra-CNS imaging. From a clinical standpoint, a key-differentiating feature of PLE from herpes encephalitis is a more insidious onset of symptoms. Clinical findings are nonspecific and include short-term memory loss, seizures, confusion, and psychiatric changes, as might be expected given involvement of the limbic system.[3]

CT again has a limited role in evaluating for limbic encephalitis and MRI is the modality of choice. As with HSE, imaging findings are nonspecific, but similarly include preferential T2/FLAIR hyperintensity within the medial temporal lobes as well as the inferior frontal regions, insula, and cingulate gyrus. Involvement of the medial temporal lobes can be unilateral or bilateral, and enhancement may be present as well **(Figure 4)**.[4]

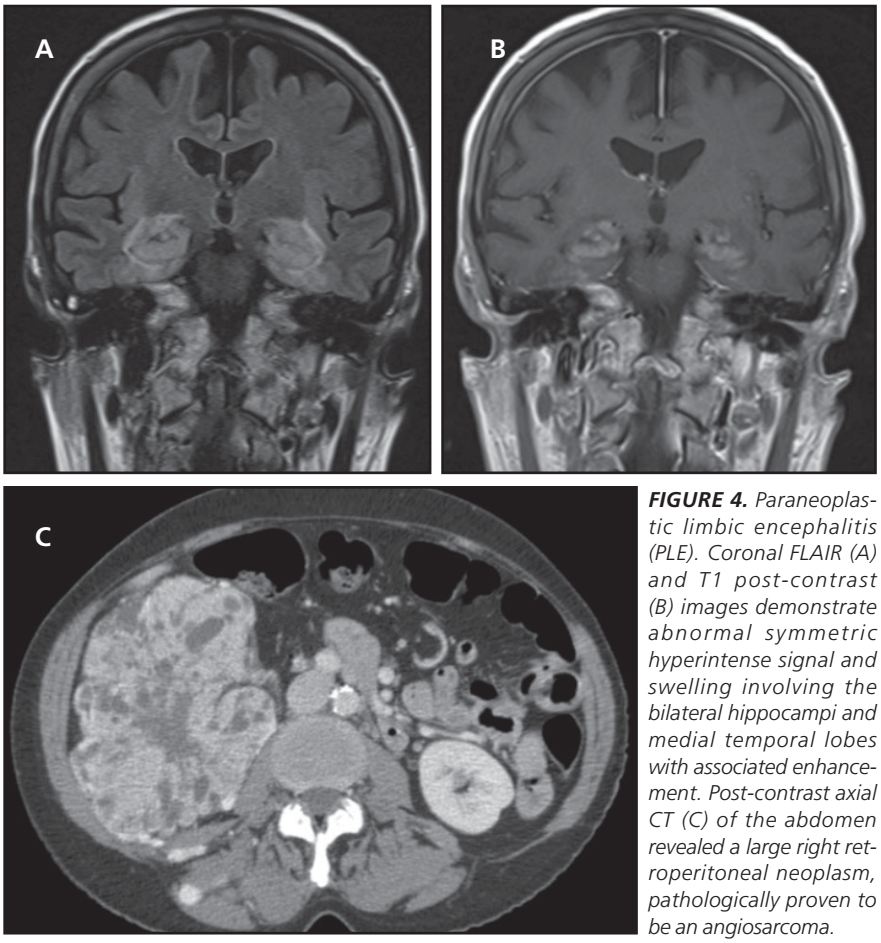

FIGURE 4. *Paraneoplastic limbic encephalitis (PLE). Coronal FLAIR (A) and T1 post-contrast (B) images demonstrate abnormal symmetric hyperintense signal and swelling involving the bilateral hippocampi and medial temporal lobes with associated enhancement. Post-contrast axial CT (C) of the abdomen revealed a large right retroperitoneal neoplasm, pathologically proven to be an angiosarcoma.*

Anti-NMDA (N-methyl-D-aspartate) receptor encephalitis is another form of autoimmune encephalitis that has gained much attention recently. This entity was originally described in adult women with underlying ovarian teratoma, but is now recognized in adult men and children even in absence of a systemic neoplasm.[5] Clinical features include an initial prodrome of fever, headache, vomiting, and diarrhea. Psychiatric symptoms include anxiety, paranoia, and insomnia. Ultimately, psychosis may develop within weeks of the prodromal phase in addition to movement disorders, seizures, cognitive decline, and autonomic dysfunction. Diagnosis is confirmed by the presence of NMDA receptor antibodies in serum or CSF.

CT has poor sensitivity for detection of this entity, and MRI is the study of choice; however, even MRI may be negative in 50% of confirmed cases. When present, MRI findings include T2/FLAIR hyperintensity within the hippocampus; cerebellar, frontobasal or insular cortex; basal ganglia; brainstem; and occasionally the spinal cord.[5] Contrast enhancement may be present within these regions of signal abnormality and occasionally, abnormal meningeal enhancement may be identified.

Recent literature suggests anti-NMDA receptor encephalitis is more common than previously recognized, but unfortunately, the diagnosis based on neuroimaging alone is very difficult. When diagnosed early, this represents a treatable form of autoimmune encephalitis. Therefore, it is important for the radiologist to be familiar with this entity when interpreting an imaging study that demonstrates findings of limbic encephalitis. While this autoimmune encephalitis may occur in the absence of systemic neoplasm, screening for ovarian teratoma in females or testicular or small cell lung carcinoma in males, should be recommended.

Gliomatosis Cerebri

Gliomatosis cerebri represents a rare, diffusely infiltrative glial neoplasm that may arise de novo, from a previous astrocytoma, or less commonly from an oligodendroglioma. These are aggressive neoplasms with WHO grades ranging from II-IV (most are WHO III).[2] By definition, at least three lobes of the brain are involved (updated WHO classification) with common extension into the basal ganglia and deep cerebral white matter. Gliomatosis can occur at any age but there is a peak presentation between ages 40 and 50.[6] Clinically, patients may present with cognitive or behavioral decline, headaches, seizures, or other focal neurologic derangement that is generally more insidious in onset than herpes encephalitis. Prognosis is poor, and given its diffusely infiltrative behavior, these are nonresectable. Chemotherapy and radiation treatment have not had a positive impact on overall survival.

CT has a limited role in evaluating for gliomatosis because the findings may be completely unapparent or at least very subtle. Potential abnormalities include hypodense regions in the white matter associated with subtle mass effect and poor gray-white differentiation. Enhancement is usually not detected on postcontrast CT.

MRI is the imaging modality of choice. Findings typically include extensive T2/FLAIR hyperintense, infiltrative signal abnormality with relatively mild associated mass effect **(Figure 5)**. T1 changes are less conspicuous with areas of signal abnormality that are iso- to hypointense relative to normal gray matter. Despite widespread infiltration of the white matter, white matter architecture is otherwise often preserved. Enhancement is absent or minimal; however, when present, areas of enhancement or restricted diffusion suggest a higher-grade tumor. In general, gliomatosis lacks the vascular proliferation and necrosis typical

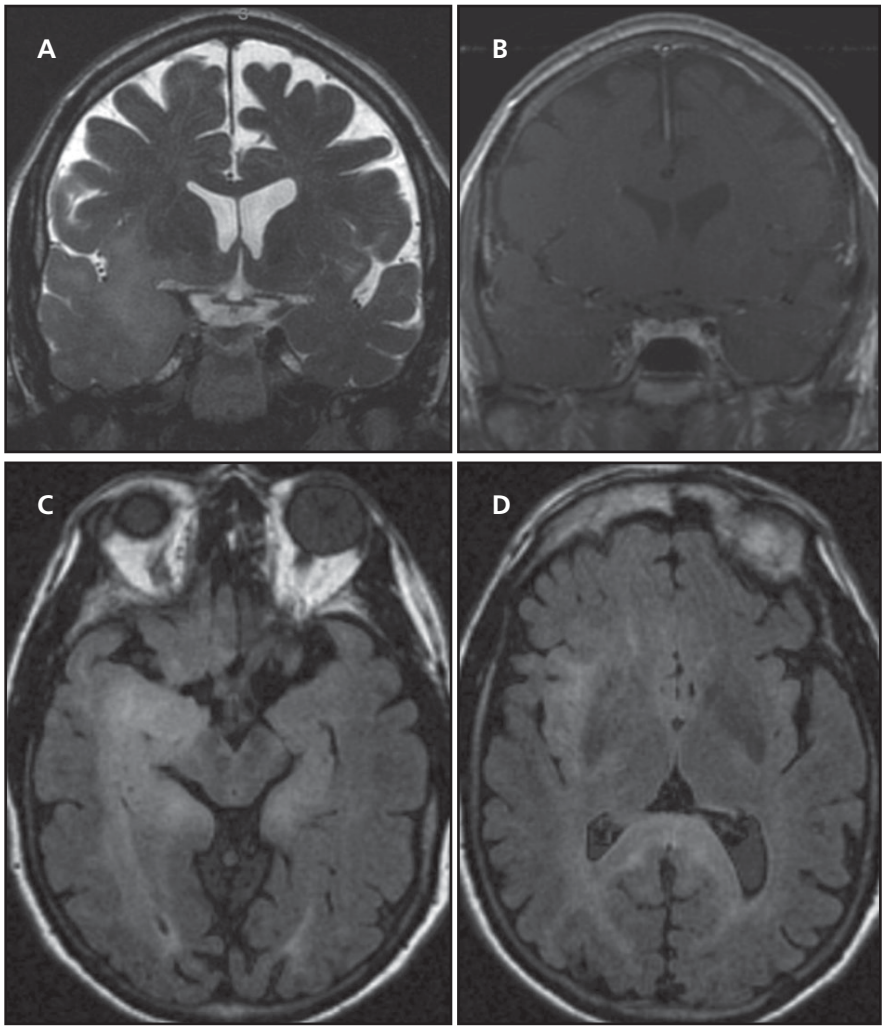

FIGURE 5. *Gliomatosis cerebri. Coronal fast multiplanar inversion recovery (FMPIR) image (A) demonstrates abnormal hyperintense signal and mild swelling involving the right insula, temporal lobe, and inferomedial frontal lobe without enhancement on postcontrast T1 (B). Axial FLAIR images (C and D) show further extent of signal abnormality to also involve the splenium and contralateral mesial temporal lobe.*

for high-grade glial neoplasms, which likely accounts for the lack of enhancement or increased rCBV (relative cerebral blood volume) on perfusion.[7] MR spectroscopy may show typical tumor-like spectra with reduced NAA (N-acetylaspartate) and elevated choline.

Peri- or Postictal Edema

Following a generalized tonic-clonic seizure or status epilepticus, transient and reversible signal changes may occur in the region of epileptic discharge. These signal changes are thought to result from vasogenic and cytotoxic edema induced by seizure activity.[8] In the acute setting, these signal changes could be mistaken for infiltrative tumor, infarction, or encephalitis. The key to this diagnosis is not only the appropriate clinical history of seizure, but also demonstrating reversibility on follow-up imaging.

CT has a limited role in evaluating parenchymal abnormalities in the setting of seizure, and MRI is again the modality of choice. Imaging features will vary based on acuity and overall severity of seizure activity. Common MRI findings include T2/FLAIR hyperintensity and swelling of involved cortical gyri, hippocampus, and occasionally the ipsilateral thalamus and basal ganglia **(Figure 6)**. The subcortical white matter may be involved to some extent, but signal abnormality tends to predominate in the cortex. Restricted diffusion is often present **(Figure 6A and 6C)**, although its reversibility suggests that cytotoxic edema alone does not account for the diffusion restriction. Increased MR perfusion and minimal enhancement may be present as well at postictal imaging **(Figure 6G)**. Most of these peri- or postictal signal abnormalities will normalize within days; however, cortical atrophy, laminar necrosis, mesial temporal sclerosis and gliosis may be identified in the chronic setting.

Infarction

Acute or subacute cerebral infarction is an important cause of gyral swelling and signal abnormality within the temporal lobe and elsewhere. Most infarcts are arterial in origin, which may result from thrombosis of vulnerable atherosclerotic plaque in a large vessel, small vessel occlusion, or cardioembolic events. As with the other entities discussed, MRI is far more sensitive than CT in detecting acute ischemia or infarction. On imaging, both gray and white matter are often involved with a thromboembolic infarct, characteristic of cytotoxic edema **(Figure 7)**. Diffusion restriction precedes T2/FLAIR signal abnormality, which is a notable differentiating feature from postictal gyral edema (in which case T2/FLAIR hyperintensity and restricted diffusion occur simultaneously). An important feature of arterial origin thromboembolic infarcts is involvement of a specific vascular territory. For the radiologist, understanding the normal cerebral arterial vascular distributions is vital. This is particularly important when temporal lobe signal abnormality is encountered since there is mixed arterial supply. Specifically, the posterior cerebral artery (PCA) supplies the inferomedial temporal lobe, the middle cerebral artery (MCA) supplies the lateral and superior temporal lobe, and the anterior choroidal artery supplies a portion of the hippocampus.

Most cerebral infarctions are "bland"

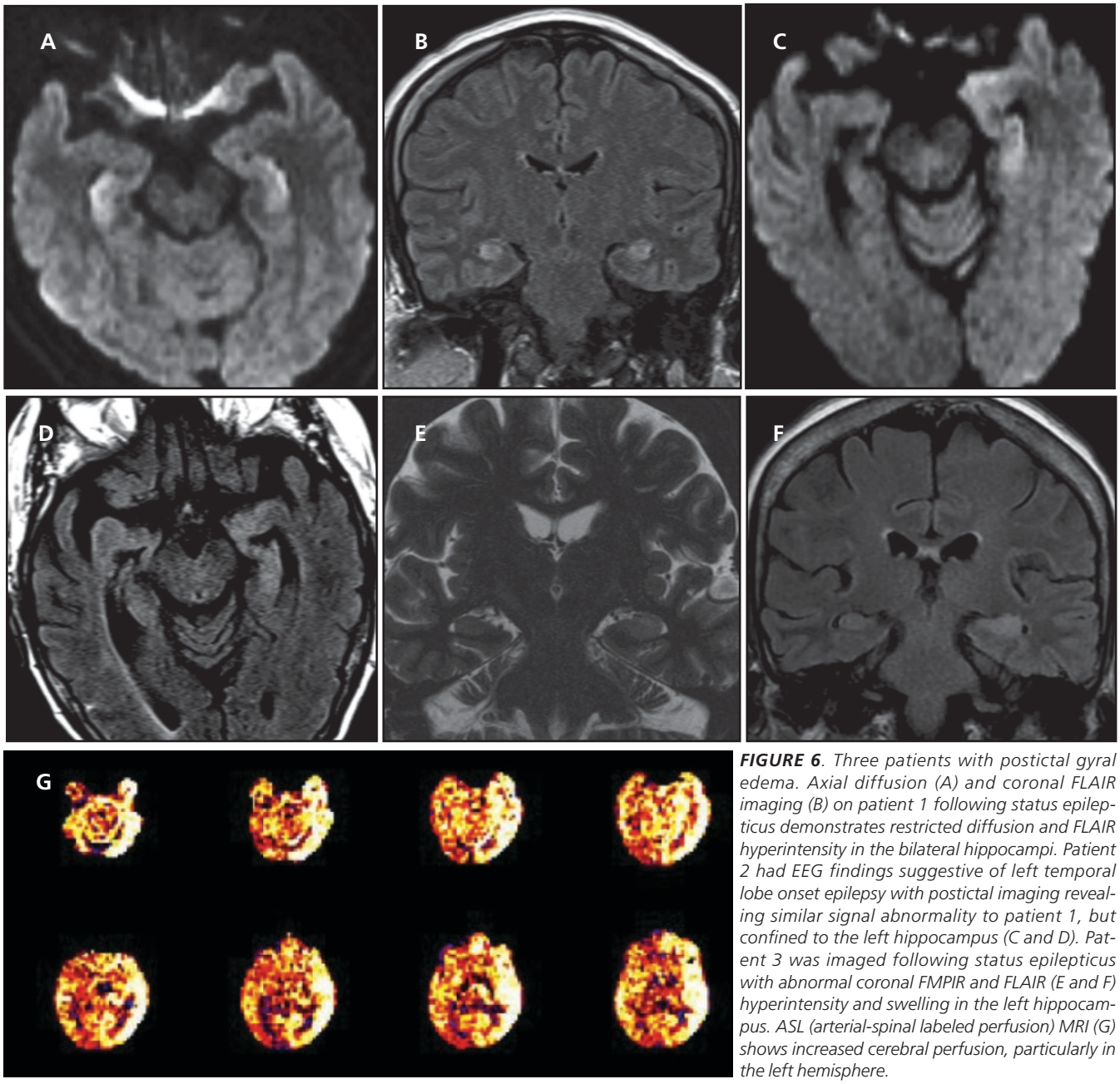

FIGURE 6. *Three patients with postictal gyral edema. Axial diffusion (A) and coronal FLAIR imaging (B) on patient 1 following status epilepticus demonstrates restricted diffusion and FLAIR hyperintensity in the bilateral hippocampi. Patient 2 had EEG findings suggestive of left temporal lobe onset epilepsy with postictal imaging revealing similar signal abnormality to patient 1, but confined to the left hippocampus (C and D). Patent 3 was imaged following status epilepticus with abnormal coronal FMPIR and FLAIR (E and F) hyperintensity and swelling in the left hippocampus. ASL (arterial-spinal labeled perfusion) MRI (G) shows increased cerebral perfusion, particularly in the left hemisphere.*

or nonhemorrhagic, but hemorrhagic transformation may complicate ischemic infarcts, usually in the first 24 hours following reperfusion therapy, or spontaneously over a few days or first week following infarct ictus. Petechial hemorrhage appears as punctate foci of hemorrhage within the cortex or basal ganglia without mass effect and likely reflects tissue reperfusion.[2] Petechial hemorrhage occurs far more frequently than parenchymal hematoma formation and generally does not alter patient prognosis or therapy. However, gross hematoma formation does carry increased morbidity and decreased survival. Spontaneous hemorrhagic transformation is seen more commonly in cardioembolic origin infarcts with additional risk factors for hematoma formation, including thrombolytic therapy, large infarcts, and hyperglycemia.

Occlusion of dural venous sinuses and/or cerebral veins is a rare cause of acute "strokes"; however, the radiologist may be the first to suggest or make the diagnosis given the elusive nature of its clinical presentation. Common patient signs and symptoms include headache (seen in 90% of patients), nausea, vomiting, seizure, and altered consciousness.[9] Veno-occlusive disease tends to affect younger individuals and is more commonly seen in females with the following risk factors: oral contraceptives, pregnancy, hypercoagulable states, dehydration, drugs, infection, and trauma (among others).

Formation of thrombus within a dural

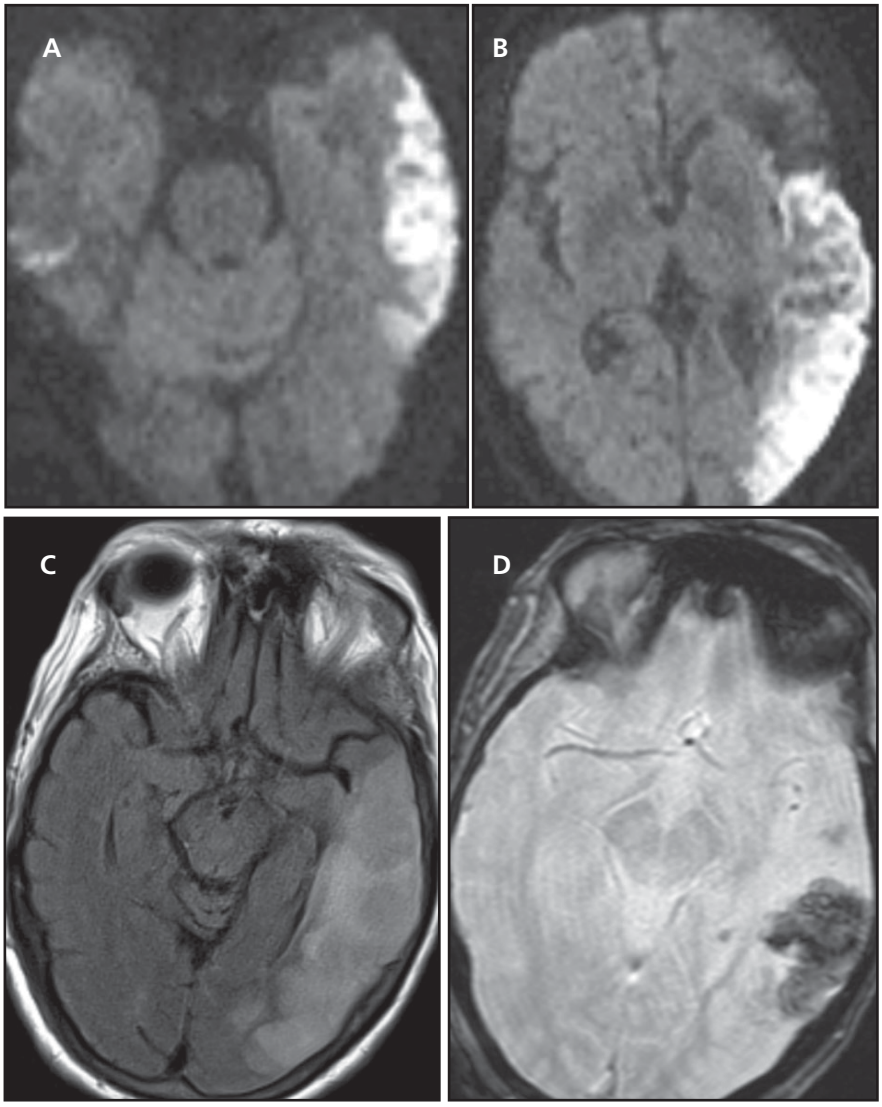

FIGURE 7. *Early subacute left MCA infarct. Axial diffusion weighted images (A and B) show restricted diffusion corresponding to the territory of the left inferior MCA division (ADC not shown). Axial FLAIR image (C) reveals associated gyral edema with loss of normal gray-white interface. Axial GRE image (D) demonstrates susceptibility artifact due to complicating hemorrhagic transformation.*

sinus, cortical vein, or deep cerebral vein impairs venous outflow. Consequently, venous pressures become elevated, resulting in venous congestion and parenchymal ischemia. Venous infarcts have a relatively high propensity for hemorrhagic transformation (30-40%), and an important distinguishing feature is that they will cross normal arterial vascular territories.[9] The region of infarct can be predicted by the dural sinus or veins occluded. For instance, superior sagittal sinus occlusion results in bilateral, parasagittal frontal, parietal and occipital lobe infarcts; transverse and sigmoid sinus occlusion results in temporal and occipital lobe infarcts; vein of Labbe occlusion results in temporal lobe infarcts; and vein of Galen or straight sinus occlusion can result in infarcts of the bilateral thalami and basal ganglia.

On noncontrast CT, a clot within the dural sinus or vein will appear hyperdense, while on MRI, the appearance of thrombus will vary depending on its age. Postcontrast imaging is very useful to detect thrombus, which appears as a "filling defect" within an otherwise opacified venous structure. CT or MR venography are also frequently utilized protocols when veno-occlusive disease is suspected clinically or to clarify findings on noncontrast imaging. It is important for the radiologist to be aware of certain imaging pitfalls that mimic venous occlusion including variant venous sinus anatomy, arachnoid granulations, or flow-related artifacts on MRI.

Diagnosis

Herpes simplex encephalitis (HSE)

Summary

Herpes simplex encephalitis (HSE) is a potentially devastating neurologic disease; therefore, it is imperative that the radiologist recognize and communicate this diagnosis to the referring clinician for urgent anti-viral therapy. Other imaging considerations that can mimic HSE include other autoimmune encephalitides, gliomatosis cerebri, postictal gyral edema, and acute cerebral infarction. Knowledge of the timing and nature of clinical presentation can assist the radiologist in differentiating these potential entities as being more or less likely.

References

1. National Institute of Neurological Disorders and Stroke. Meningitis and encephalitis fact sheet. 2004. Retrieved from http://www.ninds.nih.gov/disorders/encephalitis_meningitis/detail_encephalitis_meningitis.htm. Accessed December 22, 2014.
2. Osborn AG. *Osborn's brain: Imaging, Pathology and Anatomy, 1st ed.* Philadelphia, PA: Lippincott Williams & Wilkins, 2012.
3. Asztely F, Kumlien E. The diagnosis and treatment of limbic encephalitis. *Acta Neurol Scand* 2012; 126(6): 365-375.
4. Gultekin SH, Rosenfeld MR, Voltz R., et al. Paraneoplastic limbic encephalitis: neurological symptoms, immunological findings and tumour association in 50 patients. *Brain* 2000; 123(7):1481-1494.
5. Jones KC, Benseler SM, Moharir M. Anti-NMDA Receptor Encephalitis. *Neuroimag Clin N Am* 2013; 23: 309-320.
6. Rajz GG, Nass D, Talianski E. et al. Presentation patterns and outcome of gliomatosis cerebri. *Oncol Lett* 2012; 3(1):209-213.
7. Yang S, Wetzel S., Cha S. Dynamic contrast-enhanced T2*-weighted MR imaging of gliomatosis cerebri. *AJNR Am J Neuroradiol* 2002;23: 350-355.
8. Kim J, Chung JI, Yoon PH, et al. Transient MR signal changes in patients with generalized tonicoclonic seizure or status epilepticus: periictal diffusion-weighted imaging. *Am J Neuroradiol* 2001; 22:1149-1160.
9. Saposnik G, Barinagarrementeria F, Brown RD Jr, et al. Diagnosis and management of cerebral venous thrombosis: a statement for healthcare professionals from the American Heart Association/American Stroke Association. *Stroke* 2011; 42:1158-1192.

Lytic Epiphyseal Lesion

Hemang Kotecha, D.O., Christopher Cerniglia, D.O.

Department of Radiology, University of Massachusetts Memorial Medical Center, Worcester, MA

Case Presentation

A 44-year-old woman with a history of Sjogren syndrome presented with 4 months of right elbow pain that began spontaneously, without any known precipitating trauma or injury. She denied constitutional symptoms. Radiographs of the right elbow **(Figure 1A)** were initially interpreted as negative at an outside institution. Her pain was attributed to inflammation and perhaps tendinitis, and she was sent to physical therapy. Ultimately, the pain did not improve, and an MRI was performed **(Figures 1B-D)**.

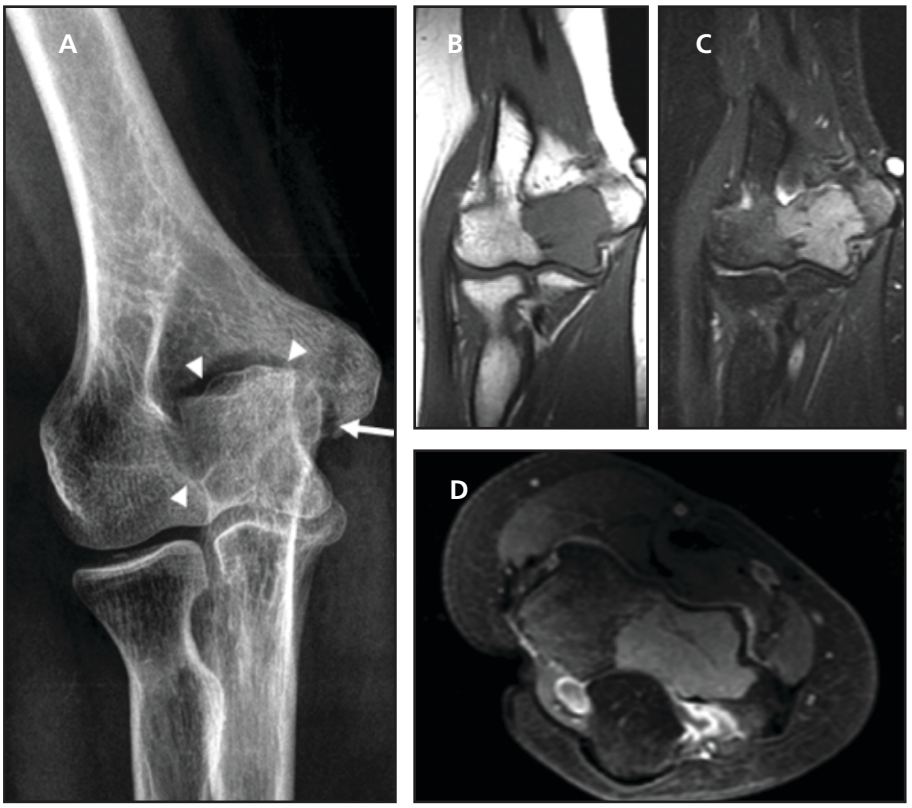

FIGURE 1. *Frontal radiograph of the right elbow (A) demonstrates a geographic lucent lesion in the epiphysis of the distal right humerus (arrowheads), extending to the trochlear articular surface (arrow). There is no periosteal reaction, cortical destruction, or evidence of soft tissue component. Coronal T1 (B) and short tau inversion recovery (STIR) (C) MR images confirm the findings on the radiograph. The lesion demonstrates intermediate T1 and intermediate high T2 signal. The extent of the lesion is limited to the epiphysis. Axial fat-suppressed T1 postcontrast image (D) demonstrates mild diffuse homogenous enhancement.*

Key Imaging Finding(s)

Solitary lytic epiphyseal intramedullary bone lesion

Differential Diagnoses

Giant cell tumor
Chondroblastoma
Clear cell chondrosarcoma
Eosinophilic granuloma

Discussion

A systematic approach is necessary in providing an accurate differential diagnosis for osseous lesions. Plain radiographs are the mainstay for characterizing these lesions, especially in terms of having an aggressive or non-aggressive appearance. Key features to identify include the zone of transition between the lesion and surrounding bone and the presence of cortical destruction or periosteal reaction. In addition, lesion location and patient demographics play a critical role in establishing a reasonable list of differential diagnoses. The leading differential diagnoses for this solitary epiphyseal intramedullary lucent lesion with a non-aggressive imaging appearance include giant cell tumor, chondroblastoma, clear cell chondrosarcoma, and eosinophilic granuloma, although infection could have a similar appearance in the appropriate clinical setting.

Giant cell tumor: Giant cell tumor (GCT) is a typically benign, locally aggressive, lytic lesion that is located eccentrically within metaphyseal bone and extends to the articular surface. Histologically, giant cell tumors contain a prominent and diffuse osteoclastic giant cell component on a background of mononuclear cells.[1] The histopathological differential diagnosis of giant cell tumor is extensive. Therefore, careful correlation between clinical, pathologic, and radiologic features is necessary for accurate diagnosis.

The majority of GCTs affect skeletally mature patients with a peak prevalence in the third decade. Approximately 80% of lesions occur in patients between 20 and 50 years of age.[1] Clinical symptoms are nonspecific and include pain, swelling, and decreased range of motion at the adjacent joint. In instances of pathologic fracture, patients may present with acute onset of pain.

Radiographically, location is the key diagnostic feature, as the vast majority extend to within 1 cm of subarticular bone. The knee is the most common site of involvement, including the distal femur and proximal tibia. On radiographs, GCTs classically exhibit geographic osteolysis, a narrow zone of transition, and non-sclerotic borders. The majority of lesions are eccentric in location; however, large lesions may appear centrally located. Computed tomography (CT) allows for improved evaluation of cortical thinning, pathologic fracture, periosteal reaction, and the absence of matrix mineralization. MRI is useful in the detection of the soft tissue extent of the tumor. The solid components of GCT demonstrate low to intermediate T1 and T2 signal intensity, differentiating this tumor from many other subarticular lesions. GCTs can also contain secondary aneurysmal bone cyst components, in which fluid-fluid levels are characteristic.

Chondroblastoma: Chondroblastomas are relatively rare, benign lucent bone lesions that most commonly involve the epiphyses of long bones. Histologically, these tumors contain mostly mononuclear cells and variable numbers of giant cells.[2] Chondroblastomas characteristically contain chondroid matrix and may contain fine granular calcifications. Similar to giant cell tumor, they may also less commonly contain aneurysmal bone cyst components. When cytologic atypia is present, chondroblastomas may have pathologic features that overlap with osteosarcoma and clear cell chondrosarcoma; in these cases, radiologic correlation is necessary to establish an accurate diagnosis.[2]

Chondroblastomas typically occur in young patients with a mean age at diagnosis of approximately 20 years, but they can occur at almost any age.[3] The incidence is greater in men compared to women. Patients often clinically present with pain, tenderness, stiffness, and swelling. Similar to GCTs, chondroblastomas most commonly occur at the knee.

The classic radiographic appearance of chondroblastoma is that of a geographic epiphyseal lucent lesion with a thin, fine sclerotic margin. Matrix mineralization is seen in approximately 30 percent of cases.[3] The majority of chondroblastomas extend into the metaphysis to some degree in patients with fused growth plates. The presence of thick, solid periosteal reaction may help differentiate this lesion from other indolent lucent lesions. On MRI, chondroblastoma typically demonstrates intermediate T1; low T2 signal; and a thin, lobular, hypointense margin. Areas of low signal are secondary to chondroid matrix mineralization. On post-contrast imaging, most lesions demonstrate either lobular or peripheral enhancement.[3] The majority of lesions show perilesional increased T2 signal and enhancement within the bone marrow and periosteal regions which reflects hyperemia and/or edema secondary to inflammatory reaction associated with elevated tumor prostaglandin levels.[4]

Clear cell chondrosarcoma: Clear cell chondrosarcoma is 1 of 5 histologic variants of chondrosarcoma, which has a strong predilection for the epiphyses of long bones. Tumor cells range from immature chondroblasts to mature chondrocytes which have neoplastic cells containing clear cytoplasm and centrally positioned nuclei. Clear cell chondrosarcoma is a slow-growing neoplasm seen in patients with closed physes and a peak incidence between 30 and 40 years of age.

Radiographically, clear cell chondrosarcoma is a lytic lesion, which may have sclerotic borders. Matrix mineralization is demonstrated in one-third of cases. Small lesions may be well-circumscribed, while larger lesions (> 3 cm) can have cortical destruction and soft tissue extension. Clear cell chondrosarcoma shows intermediate low T1 and intermediate high T2 signal with heterogeneous enhancement.

When matrix mineralization is present, internal low T1 and T2 signal is often present.

Eosinophilic granuloma: Langerhans cell histiocytosis (LCH) is a disease that encompasses 3 clinical syndromes, including eosinophilic granuloma (EG), Hand-Schüller-Christian disease, and Letterer-Siwe disease. The most common manifestation is eosinophilic granuloma, which is a localized and usually solitary benign bone lesion. The exact etiology is unknown, but the pathogenesis involves a proliferation and – in aggressive forms – dissemination of the Langerhans cells (LC). In EG, the bone is destroyed and replaced by LCs and numerous eosinophils.[5]

Patients with EG present clinically with pain and swelling with or without soft tissue mass. Although most patients manifest symptoms prior to age 15, patients can be affected at nearly any age. Symptoms vary depending on the site of osseous involvement; many patients may even be asymptomatic. While any bone may be involved, EG has a predilection for flat bones, most frequently affecting the skull. Approximately one-third of lesions involve long bones, of which the femur is the most common. Within the long bones, most lesions are found in the diaphysis, followed by the metaphysis; epiphyseal lesions are rare. Lesions may cross the growth plate.[5]

EG can have a variety of radiographic appearances. In the acute phase, they are aggressive-appearing lytic lesions with a wide zone of transition and may be difficult to differentiate from Ewing sarcoma or infection. Chronic lesions in long bones may also vary in appearance with some lesions presenting as a small area of medullary destruction with well-defined sclerotic margins. Other lesions may progress, causing endosteal scalloping, cortical destruction, and a soft tissue mass.[5] CT is useful in delineating the extent of the lesion, presence of a soft tissue mass, and degree of cortical destruction. MRI has similar benefits, although the imaging characteristics on both modalities may be nonspecific and overlap with more aggressive lesions.

Diagnosis

Giant cell tumor

Summary

Key features to assess in determining the aggressiveness of a bony lesion include the zone of transition, presence of cortical destruction, and periosteal reaction. Once the aggressiveness of the lesion has been established, the differential diagnosis depends largely on patient age and gender, as well as lesion location, multiplicity, and matrix calcifications. In our patient scenario, the lesion location and imaging characteristics were essential to establishing an appropriate differential diagnosis for an epiphyseal lesion. As with most cases, the final diagnosis was made based on a combination of the clinical presentation, imaging characteristics, and pathologic assessment.

References

1. Murphey MD, Nomikos GC, Flemming DJ, et al. Imaging of giant cell tumor and giant cell reparative granuloma of bone: radiologic-pathologic correlation. RadioGraphics 2001; 21:1283-1309.
2. Qasem SA, DeYoung BR. Cartilage-forming tumors. Semin Diagn Pathol 2014; 31(1):10-20.
3. Douis H, Saifuddin A. The imaging of cartilaginous bone tumors. I. Benign lesions. Skeletal Radiol 2012; 41:1195-1212.
4. Yamamura S, Sato K, Sugiura H, et al. Prostaglandin levels of primary body tumor tissues correlate with peritumoral edema demonstrated by magnetic resonance imaging. Cancer 1997; 79:255-261.
5. Azouz EM, Saigal G, Rodrigues MM, Podda A. Langerhans' cell histiocytosis: pathology, imaging, and treatment of skeletal involvement. Pediatr Radiol 2005; 35:103-115.

JAOCR at the Viewbox

Aaron Betts, M.D.

Department of Radiology, Cincinnati Children's Hospital Medical Center, Cincinnati, OH

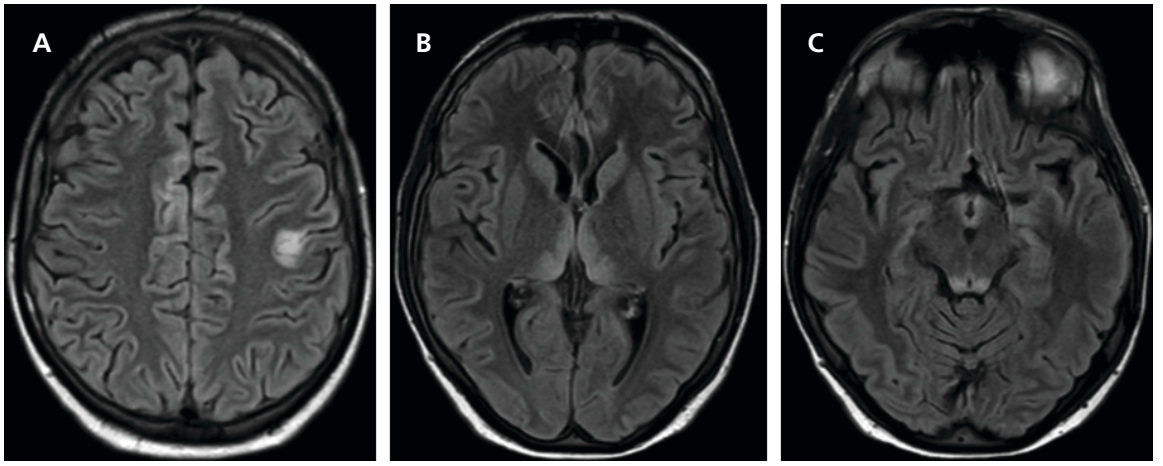

Wernicke Encephalopathy

An 18-year-old critically ill boy was receiving parenteral nutrition during a complicated hospitalization. MRI was obtained after he developed a decreased level of alertness and twitching in his right arm. Axial fluid-attenuated inversion recovery (FLAIR) images showed hyperintense signal involving the cortex of the posterior left frontal lobe, posteromedial thalami, tectal plate, and mammillary bodies. Diffusion-weighted images showed corresponding diffusion restriction (not shown). Findings were consistent with nonalcoholic Wernicke encephalopathy. Laboratory evaluation confirmed thiamine deficiency, and he underwent intravenous thiamine repletion; his mental status changes and right upper extremity twitching subsequently resolved.

Wernicke encephalopathy is caused by thiamine (vitamin B1) deficiency. The classic triad of Wernicke encephalopathy consists of altered consciousness, ophthalmoplegia, and ataxia. Typical areas of involvement include the mammillary bodies, periaqueductal gray matter, tectal plate, and medial thalami. Atypical areas include the cerebellum, caudate nuclei, red nuclei, splenium, and cerebral cortex.[1] MR signal abnormalities in these areas show increased T2 and FLAIR signal, often with diffusion restriction.

In adults, Wernicke encephalopathy is commonly associated with chronic alcoholism. In nonalcoholic patients, numerous causes of nutritional deficiency of thiamine can lead to Wernicke encephalopathy in both pediatric and adult patients, including parenteral nutrition, hyperemesis from pregnancy or chemotherapy, eating disorders, and poor nutrition secondary to poverty or neglect.[2] Without treatment, Wernicke encephalopathy can lead to devastating neurologic impairment or death. After treatment with intravenous repletion of thiamine, the imaging findings and neurologic symptoms of Wernicke encephalopathy are often reversible.[1,2]

1. Ha ND, Weon YC, Jang JC, et al. Spectrum of MR imaging findings in Wernicke encephalopathy: are atypical areas of involvement only present in nonalcoholic patients? Am J Neuroradiol 2012; 33(7):1398-1402.
2. Zuccoli G, Gallucci M, Capellades J, et al. Wernicke encephalopathy: MR findings at clinical presentation in twenty-six alcoholic and nonalcoholic patients. Am J Neuroradiol 2007; 28(7):1328-1331.

JAOCR at the Viewbox

Chelsea Sheeler, D.O., Rocky Saenz, D.O.

Department of Radiology, Botsford Hospital, Farmington Hills, MI

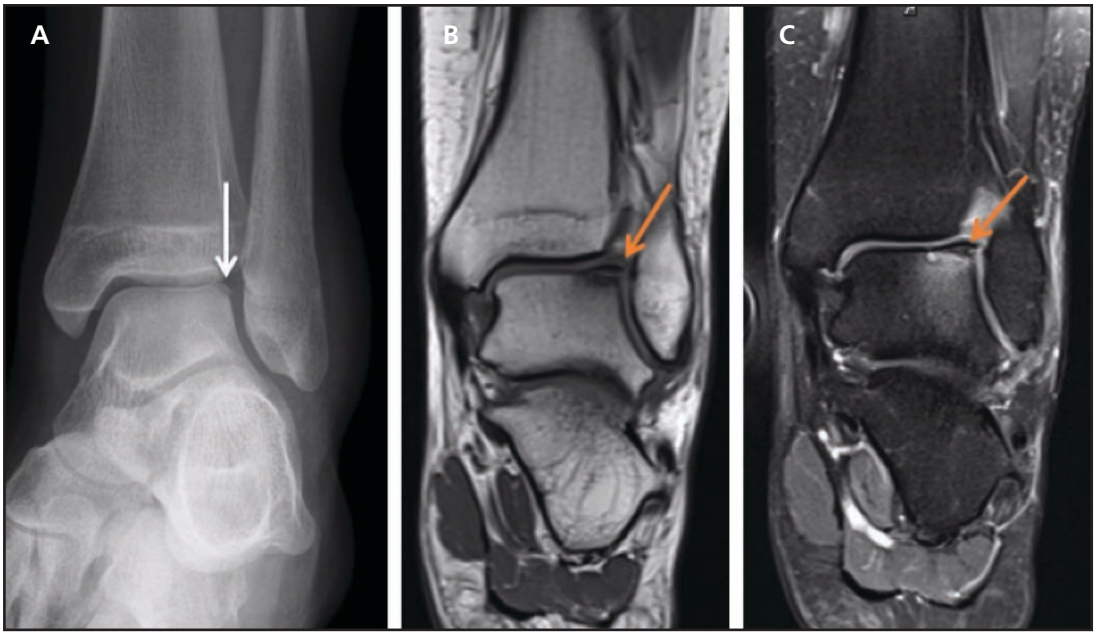

Osteochondral Defect, Unstable

A young adult patient presented with continued pain following an ankle injury despite conservative management. Radiograph of the left ankle (A) demonstrates a cortical defect with separation of an osseous fragment from the lateral talar dome (arrow). Coronal T1 (B) and proton density (PD) with fat suppression (C) images show the focal defect (arrows) with associated low T1 signal and high signal on PD between the articular cartilage and subchondral bone.

Osteochondral defect (OCD) of the talus occurs when an isolated fragment of articular cartilage and subchondral bone are detached, resulting in a loose body. Trauma remains the primary etiology secondary to acute traumatic event or repetitive loading injuries. Symptomatic OCD typically presents with chronic ankle pain, stiffness, and/or catching. Radiographic findings may initially be negative or underestimate the extent of injury. Thus, MRI is considered the modality of choice, particularly in determining instability and indications for orthopedic intervention. Stable fragments will show decreased signal intensity involving the junction of the fragment and subchondral bone on T2 sequences, which indicates healing. Unstable lesions have interposed high signal on T2 sequences, as in this case. Viability of the fragment can be assessed on T1 sequences. Necrosis is evident when the fragment has low T1 signal intensity on all sequences or does not enhance.[1]

1. Rosenberg ZS, Beltran J, Bencardino JT. MR imaging of the ankle and foot. *RadioGraphics* 2000; 20:S153-179.